Theoretical and Applied Climatology (2020) 139:1569–1588
https://doi.org/10.1007/s00704-019-03053-x

ORIGINAL PAPER

Statistical bias correction of regional climate model simulations for climate change projection in the Jemma sub-basin, upper Blue Nile Basin of Ethiopia

Gebrekidan Worku[1,2] · Ermias Teferi[1] · Amare Bantider[3,4] · Yihun T. Dile[5]

Received: 31 March 2019 / Accepted: 14 November 2019 / Published online: 17 December 2019

Abstract

This study evaluates bias correction methods and develops future climate scenarios using the output of a better bias correction technique at the Jemma sub-basin. The performance of different bias correction techniques was evaluated using several statistical metrics. The bias correction methods performance under climate condition different from the current climate was also evaluated using the differential split sample testing (DSST) and reveals that the distribution mapping technique is valid under climate condition different from the current climate. All bias correction methods were effective in adjusting mean monthly and annual RCM simulations of rainfall and temperature to the observed rainfall and temperature values. However, distribution mapping method was better in capturing the 90th percentile of observed rainfall and temperature and wet day probability of observed rainfall than other methods. As a result, we use the future (2021–2100) simulation of RCMs which are bias corrected using distribution mapping technique. The output of bias-adjusted RCMs unfolds a decline of rainfall, a persistent increase of temperature and an increase of extremes of rainfall and temperature in the future climate under emission scenarios of Representative Concentration Pathways 4.5, 8.5 and 2.6 (RCP4.5, RCP8.5 and RCP2.6). Thus, climate adaptation strategies that can provide optimal benefits under different climate scenarios should be developed to reduce the impact of future climate change.

1 Introduction

Global climate models (GCMs) are essential to study changes in the climate of the earth and to make climate change projections (Edwards 2011; Intergovernmental Panel on Climate Change (IPCC) 2013). Since mainly the 1950s, GCMs are under development and there are vital improvements. For instance, the Earth System Modelling Framework is the most essential step in climate modelling (Taylor et al. 2012; Edwards 2011). In fifth phase of Climate Model Intercomparison Project (CMIP5), several GCMs have been developed into Earth System Models by incorporating the representation of biogeochemical cycles (Taylor et al. 2012). Better than the earlier phases of IPCC models, the atmosphere and the ocean components of CMIP5 models have higher spatial resolution (Taylor et al. 2012; Woldemeskel et al. 2015; Yang et al. 2018). Consequently, CMIP5 GCMs reproduce the global scale mean surface temperature and the seasonal cycle of sea ice extent of oceans (Flato et al. 2013; Taylor et al. 2012).

Despite several improvements, CMIP5 GCMs perform less effectively in simulating cloud cover and rainfall of mountainous and coastal regions (Randall et al. 2007; Flato et al. 2013; Woldemeskel et al. 2015; Yang et al. 2018). Model parameterization, greenhouse emission scenarios, and internal climate variability are the key sources of uncertainties in GCMs (IPCC 2013). Low spatial resolution of GCMs is another source of uncertainty that hiders GCMs to reproduce the local

Electronic supplementary material The online version of this article (https://doi.org/10.1007/s00704-019-03053-x) contains supplementary material, which is available to authorized users.

✉ Gebrekidan Worku
gebrwor@dtu.edu.et

[1] Centre for Environment and Development Studies, Addis Ababa University, Addis Ababa, Ethiopia

[2] Department of Natural Resources Management, Debretabor University, Debra Tabor, Ethiopia

[3] Centre for Food Security Studies, Addis Ababa University, Addis Ababa, Ethiopia

[4] Water and Land Resources Centre, Addis Ababa University, Addis Ababa, Ethiopia

[5] College of Agriculture and Life Sciences, Texas A&M University, College Station, TX, USA

and regional scale climate specially in the mountain and coastal regions (Fowler et al. 2007). Thus, downscaling of GCM simulation at the regional-scale is important for local climate impact studies (Wilby 1997; Flato et al. 2013). Yet again, downscaling GCMs simulation to the local scale is another vital source of uncertainty and as a result it is crucial to select a better downscaling technique. Statistical and dynamical downscaling are primary downscaling techniques that produce regional and local scale climate data from GCMs (Wilby et al. 2002). There are evidence which unfold dynamical downscaling is superior than statistical downscaling techniques to simulate rainfall of regions with diverse topography (Fowler et al. 2007).

Using the dynamical downscaling approach, there are international programs that use the third and fifth phases of CMIP (CMIP5 and CMIP5) to project the future climate (Christensen and Carter 2007; Giorgi et al. 2009; Mearns et al. 2013; Gutowski et al. 2016). Under the auspice of the World Climate Research Program (WCRP), the Coordinated Regional Climate Downscaling Experiment (CORDEX) is an international program to avail downscaled climate dataset, to integrate model evaluation frameworks and to use climate models data for climate change impact studies (Giorgi et al. 2009). The outputs of CORDEX are evaluated and used for climate change impact studies in different parts of Africa and showed reasonable standard (Nikulin et al. 2012; Dosio et al. 2015; Haile and Rientjes 2015). But, as yet the output of downscaled RCMs showed persistent biases and cannot be directly used without tailoring and bias correction for climate change impact assessment (Piani et al. 2010; Gudmundsson et al. 2012; Yang et al. 2018).

Bias correction is the science of scaling climate model values to reflect the statistical properties such as mean, variance or wet-day probabilities of observed climate (Teutschbein and Seibert 2012; Maraun 2016). There are several bias correction methods; some of these methods such as linear scaling adjust only the mean of climate model simulation, whereas other methods like distribution mapping and power transformation correct the mean and frequency of models' values with the statistical values of observations (Teutschbein and Seibert 2012). Compared to others bias correction methods, distribution mapping is a better bias correction technique in adjusting frequency of rainfall and temperature events (Teutschbein and Seibert 2012; Fang et al. 2015; Azmat et al. 2018).

However, bias correction techniques have some limitations and even on some instances bias correction methods trigger biases. For instance, the bias-corrected Weather Research and Forecasting (WRF) RCM has presented larger wet bias than the non-bias-corrected WRF simulation over Canada and Central North America (Wang and Kotamarthi 2015). Another limitation of bias correction is their strong dependence on the quality of observation data (Addor and Seibert 2014). Commonly, most bias correction methods consider biases and bias correction algorithms are stationary over time (Piani et al. 2010; Maraun 2012). Nonetheless, there are studies which investigate the non-stationarity of bias correction functions (Maraun 2012). These limitations did not inhibit the application of bias correction methods since climate models are characterized by biases and can trigger considerable errors in impact assessment studies. Therefore, strong bias correction methods are to be identified before using bias corrected climate models output for future climate change impact assessment.

Several climate change impact studies in the Blue Nile Basin were based on GCM output instead of RCMs (Beyene et al. 2010; Setegn et al. 2011; Adem et al. 2016). In some studies, a single GCM output was used (e.g. Dile et al. 2013; Abdo et al. 2009). While, climate change scenarios developed based on multiple GCMs, RCMs, emission scenarios and statistical bias correction methods are lacking. It had been in limited research that bias correction was applied to study the impact of climate change at the basin scale (e.g. Elshamy et al. 2009; Liersch et al. 2016). And, this is often hardly attainable to use the output of those studies at the watershed and sub-basin level, since there is dissimilar topography and climate in the upper catchments of Blue Nile Basin. For example, rainfall trend study in the Blue Nile Basin showed different trends of historical rainfall at different sub-basins (Taye et al. 2015). This suggests the need to advance climate models pre-processing that can be used for climate change impact assessment on agriculture and water resources at every area of the Upper Blue Nile Basin.

Similar to large areas of Ethiopia, the economy of the inhabitants of the Jemma sub-basin is heavily dependent on rain-fed agriculture which is affected by the adverse impacts of climate change (Conway and Schipper 2011). In the region of Jemma, it had been studied that climate change and variability has caused drought, flooding, frost and significant loss of crops production (Tesso et al. 2012). The water resource base of the sub-basin is also highly reliant on rainfall. Rainfall contributes to 55% and 57% of runoff at the Andittid and Beressa catchments of the Jemma sub-basin respectively (Hurni et al. 2005; Gebrehiwot and Ilstedt 2011). This means variation in rainfall may trigger tremendous impacts on the water resource base and agricultural production of the sub-basin.

Thus, it is critical to develop strong climate change information that can be used for hydrological climate change impact assessment and to build optimal adaptation decisions in the water resource sector of the sub-basin. This study is planned to evaluate the performance of different bias correction methods in adjusting the RCM rainfall and temperature with observed rainfall and temperature. It is also intended to project future climate scenarios using the output of bias correction method which perform better during the historical

period at the Jemma sub-basin of Upper Blue Nile Basin. This study will support decision making in watershed and water resource-based climate change adaptation strategies.

2 Materials and methods

2.1 The study area

Jemma sub-basin with an area of about 15,000 km^2 is located in the Central Highlands of Ethiopia, Upper Blue Nile Basin (Fig. 1). The northern areas of the Jemma sub-basin are characterized by low mean annual rainfall (697 mm) whereas the high elevation areas in the north-eastern part of the sub-basin receive high mean annual rainfall (1475 mm) from 1981 to 2014. There are areas of the sub-basin with relatively low mean annual temperature (9 °C) and in contrast, there are areas with high mean annual temperature (24 °C). Increasing trends of annual and summer rainfall and a decline in spring rainfall was observed in Jemma sub-basin from 1981 to 2014. The sub-basin was also characterized by an increase in extreme rainfall and temperature events from 1981 to 2014 (Worku et al. 2018a). The main rainfall season is summer (June to September) and spring (March to May) is minor rainfall season.

The main form of livelihood in the sub-basin is smallholder mixed agriculture (i.e. cultivation of crops and domestication of livestock). Wheat, Barley, Teff, Maize and Sorghum are the main crops cultivated in the study area. High degree of land degradation and low crop yield and production which is usually less than 2 t/ha are among problems of the study area (SCRP 2000).

2.2 Observation data

Historical (1981–2005) daily rainfall and temperature data of nine climatic stations was obtained from the National Meteorological Agency of Ethiopia. These nine climatic stations (Fig. 1) have data with relatively minimal missing values, which range from 6 to 17% from 1981 to 2005. Multivariate Imputation by Chained Equations (MICE) package, built in the R statistical software (R Development Core Team, 2015), was used to impute the incomplete rainfall and temperature records. RClimDex was used to examine the quality of the data and to manage outlier values of rainfall and temperature. Detail description of missing values imputation and quality control of the data are given by Worku et al. (2018a).

2.3 Regional climate models data

In this study, the RCMs are selected based on Worku et al. (2018b) which has investigated that CCLM and REMO regional models driven by four CMIP5 GCMs were better to capture the mean and frequency of rainfall events of the Jemma sub-basin than regional climate model (RCA). However, differences still exist between the historical simulation of RCMs and observed data. Moreover, RCM performance in simulating the observed rainfall was different at different altitude (Worku et al. 2018b). This indicates the need for bias adjustment of RCM simulation at different locations. In this study, historical (1981–2005) and future (2021–2100) simulation of daily rainfall, maximum temperature (TMAX) and minimum temperature (TMIN) of CCLM and REMO models driven by four CMIP5 GCMs (Table 1) were

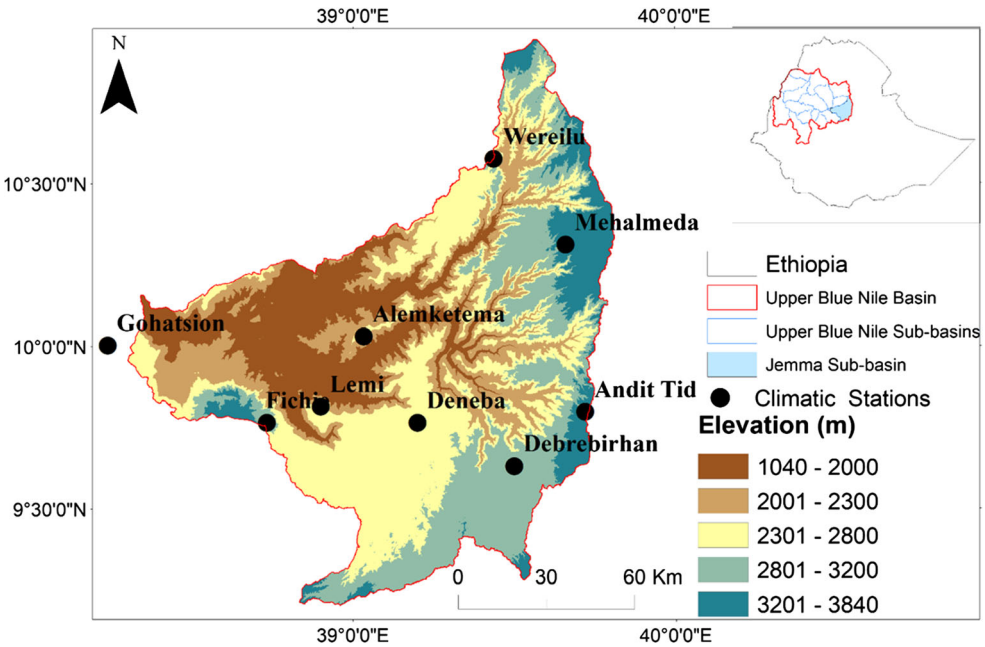

Fig. 1 Map of the Jemma sub-basin and climatic stations with elevation data as a background. The elevation map is based on the DEM data of 30 m resolution obtained from the Shuttle Radar Topographic Mission (SRTM) (http://earthexplorer.usgs.gov/)

Table 1 Detailed description of RCMs used in this study

Model acronym	CCLM(CNRM-CM5)	CCLM(EC-EARTH)	CCLM(HadGEM2-ES)	CCLM(MPI-ESM-LR)	REMO (EC-EARTH)	REMO(MPI-ESM-LR)
Driving GCM	CNRM-CM5	EC-EARTH	HadGEM2-ES	MPI-ESM-LR	EC-EARTH	MPI-ESM-LR
RCM	CCLM	CCLM	CCLM	CCLM	REMO	REMO
Institute	Climate Limited-Area Modelling (CLM) Community	Climate Limited-Area Modelling (CLM) Community	Climate Limited-Area Modelling (CLM) Community	Climate Limited-Area Modelling (CLM) Community	Max Planck Institute (MPI)	Max Planck Institute (MPI)
Resolution	0.44°	0.44°	0.44°	0.44°	0.44°	0.44°
Convective scheme	Tiedtke 1989	Tiedtke 1989	Tiedtke 1989	Tiedtke 1989	Tiedtke 1989	Tiedtke 1989
Radiation scheme	Ritter and Geleyn 1992	Ritter and Geleyn 1992	Ritter and Geleyn 1992	Ritter and Geleyn 1992	Fouquart and Bonnel (1980)	Fouquart and Bonnel (1980)
Cloud microphysics scheme	Baldauf et al. (2011)	Baldauf et al. (2011)	Baldauf et al. (2011)	Baldauf et al. (2011)	Lohmann and Roeckner, 1996@@	Lohmann and Roeckner, 1996
Land surface scheme	Doms et al. 2011	Doms et al. 2011	Doms et al. 2011	Doms et al. 2011	Rechid et al. 2009	Rechid et al. 2009

considered for statistical bias correction. Totally, the output of six RCMs was used (Table 1). The RCM data was acquired from the Earth System Grid Federation dataset (https://esgdn1.nsc.liu.se/esgf).

COSMO-CLM is the coupling of COSMO (COnsortium for Small-scale MOdelling) of different European national weather services and CLM (Climate Limited-area Model) of the German Climate Research Centre (Rockel et al. 2008). CCLM is non-hydrostatic model (Baldauf et al. 2011), whereas REMO is a hydrostatic three-dimensional atmospheric model initiated at the Max Planck Institute for Meteorology (Jacob et al., 2007). The physical parameterizations of CCLM and REMO models are given in Table 1.

After obtaining observed and historical RCM rainfall and temperature data, the observed data (point data) were interpolated to 0.44° × 0.44° grid size through the bilinear interpolation method. This is because the RCM data is gridded data (0.44° × 0.44°). To estimate sub-basin wide areal rainfall and temperature of both observation and RCMs, the Thiessen Polygon method (Theissen, 1911) was applied. Areal observed and RCM rainfall and temperature was calculated based on the area of the polygon and the grids in proportion to the total area of the sub-basin. Some of the grids of RCMs partially extend over the study area.

In each RCM, simulations based on emission scenarios of RCP4.5, RCP8.5 and RCP2.6 were used. RCP 4.5 and RCP 8.5 were selected because these emission scenarios represent possible radiative forcing levels in the year 2100 relative to pre-industrialisation (Van Vuuren et al. 2011). RCP8.5 represents high emission scenarios with increasing radiative forcing pathway resulting 8.5 W/m^2 by 2100, while RCP 4.5 represents intermediate emission levels of 4.5 W/m^2 that could be reached at stabilization after 2100 (Moss et al. 2010). In the Paris agreement, nations were agreed to limit global warming well below 2 °C (UN 2015). Therefore, RCP2.6 was used to account for the Paris Agreement and other sustainable and substantial measures to mitigate future climate change. However, CCLM4 community have downscaled only the RCP4.5 and RCP8.5. Thus, this study has used only REMO (EC-EARTH) and REMO(MPI-ESM-LR) to develop climate scenarios under RCP2.6 emission scenario.

2.4 Statistical bias correction procedures

Distribution mapping, linear scaling, variance scaling (for temperature) and power transformation (for rainfall) are the bias correction techniques which were used to adjust historical simulations of rainfall and temperature of six RCMs to the values and distribution of observed rainfall

and temperature (1981–2005). The methods find a function h that fits a modelled variable V_m such that its new values equals the values of the observed values V_o (Piani et al. 2010; Gudmundsson et al. 2012). This function can be expressed as:

$$V_o = h(V_m) \quad (1)$$

Linear scaling method (Lenderink et al. 2007) adjusts rainfall and temperature of RCM simulation using multiplicative and additive factors, respectively. The factors are developed by comparing the observed data with the corresponding historical RCM simulations. Linear scaling method corrects biases in mean but has limitations in correcting biases in probability of wet-days and intensities. Different from linear scaling, power transformation method reproduce the standard deviation, coefficient of variation (CV), wet-day frequencies and intensities of rainfall based on observed data (Leander and Buishand 2007). In power transformation, daily rainfall of RCMs is changed into a corrected rainfall through fitting the CV of the corrected daily RCM rainfall with the CV of observed daily rainfall for each month. Parallel to power transformation, variance scaling was used to fit RCM simulation of temperature (Chen et al. 2011).

In distribution mapping method, the distribution function (CDF) of RCM-simulated rainfall and temperature values are adjusted with the CDF of observed rainfall and temperature values. Distribution mapping method adjusts the mean, standard deviation, extremes and distribution of rainfall and temperature events of RCM outputs (Teutschbein and Seibert 2012). Distribution mapping uses the Gamma distribution (Gudmundsson et al. 2012) and the Gaussian distributions (Cramér 1999) to fit distribution of rainfall and temperature of RCMs with observational data. Distribution mapping also uses an RCM-specific rainfall threshold (Schmidli et al. 2006) to adjust the wet day frequencies of daily rainfall (Fig. 2). In the distribution mapping, the transformation between for instance observed rainfall and modelled rainfall is given as:

$$V_o = F_o{-}1(F_m(V_m)) \quad (2)$$

where

V_o is observed variable,
Vm is modelled variable,
Fm is the CDF related to V_m and
F_o^{-1} is the inverse CDF of V_o (Gudmundsson et al. 2012).

This study has used the CMhyd tool (Rathjens et al. 2016) to execute the bias correction techniques. The tool compares the raw RCM output with observed data, calculates the variation between observed and RCM simulated data and applies different bias correction methods to correct historical and future climate model output. The bias correction algorithms derived from historical RCM simulation and observed data were applied for the bias correction of future RCM simulation.

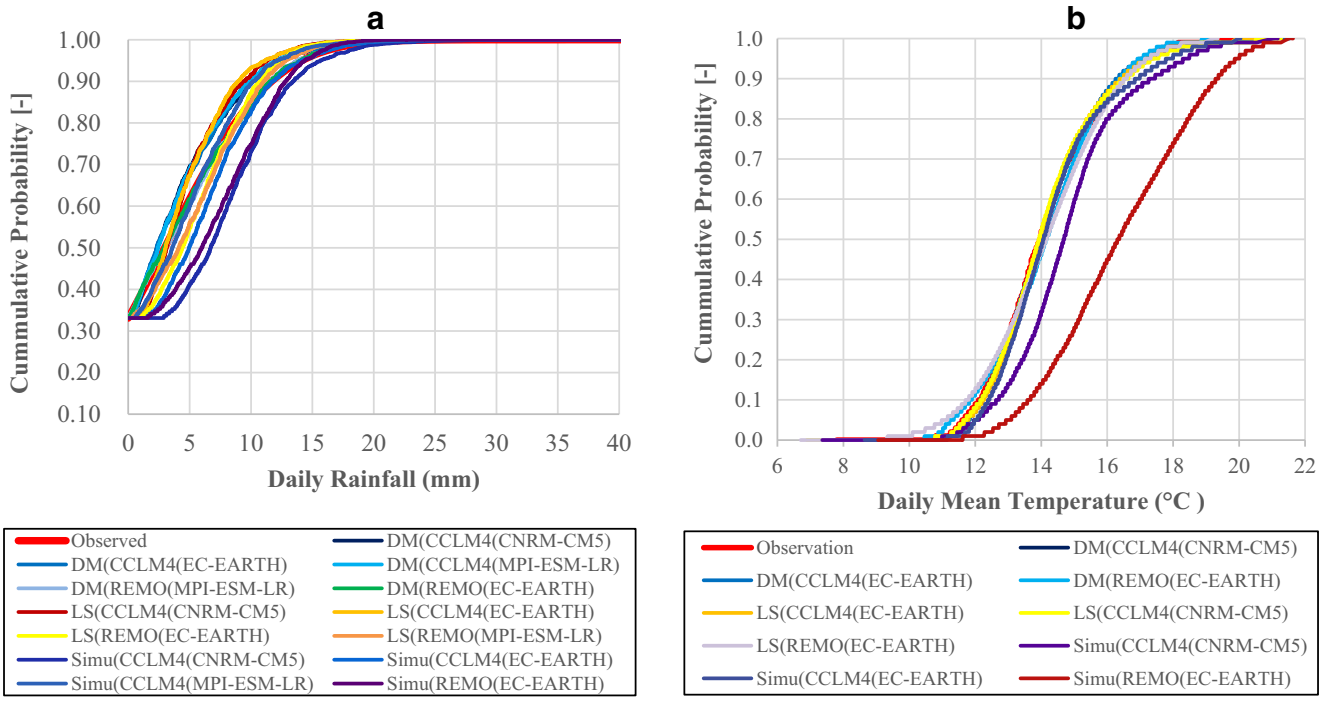

Fig. 2 Cumulative distribution of observed, RCMs simulated (Simu) and bias-corrected daily rainfall (**a**) and temperature (**b**) in Jemma sub-basin. DM and LS are distribution mapping and linear scaling bias correction methods, respectively

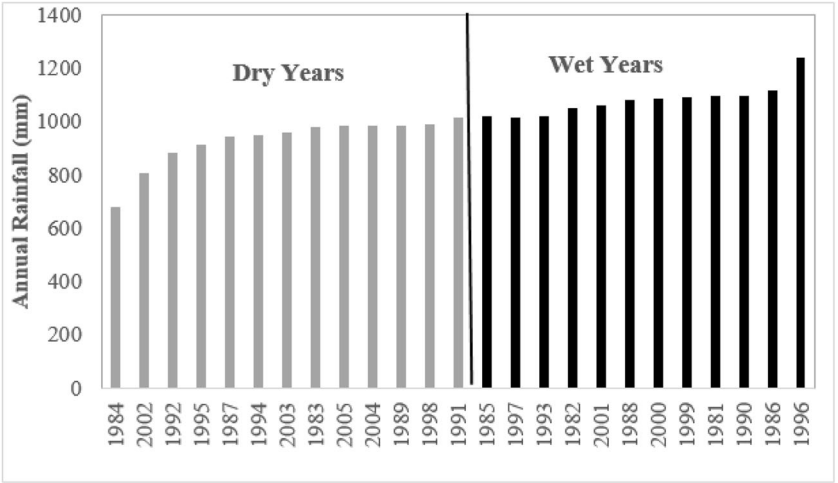

Fig. 3 Observation years sorted based on annual rainfall (1981–2005) for differential split-sample testing (DSST)

There are different approaches to test the assumption of stationarity of biases and bias correction functions (Klemeš 2016; Teutschbein and Seibert 2013). To test how distribution mapping, power transformation and linear scaling methods work for future climate condition, this study used the differential split-sample testing (DSST) method (Klemeš 2016). The following procedures of DSST were followed: first, based on observed mean annual rainfall, observed years (1981–2005) were sorted by ascending order (Fig. 3). Second, based on observed mean annual rainfall, the observed years were divided as dry years (the first 12 years) and wet years (the last 12 years), and thirdly, the RCM-simulated rainfall was sorted and rearranged to match with the annual order of the sorted observed rainfall. Then, twofold cross-validation was performed. In the first case, bias correction was executed using the dry years as calibration and wet years as validation. Secondly, bias correction was executed using the wet years as calibration and dry years for validation. A similar procedure was followed to evaluate temperature bias correction methods where the mean annual TMAX and TMIN of observed data and RCM data was sorted and divided as cold years and warm years.

The performance of bias correction methods at calibration and validation stages was tested using different metrics. The Nash–Sutcliffe measure of efficiency (NSE) and the root mean square error (RMSE) were used to test the volumetric variation between mean monthly and annual observation, RCM simulation and bias-corrected RCM outputs. Frequency-based tests which include CV, 90th percentile (X90) and the probability of wet day (Pr_{wet}) (for rainfall) were also used to evaluate the skill of bias correction methods. The bias correction method which performs better during the historical period was used to correct the RCM simulation of near-term future (2021–2050) and long-term future (2071–2100).

2.5 Future rainfall and temperature extremes analysis

The RClimDex 1.1 package (Zhang and Yang 2004) has been applied to calculate future rainfall and temperature extreme indices. Twenty-seven rainfall and temperature extreme indices were developed by the Expert Team on Climate Change Detection and Indices (ETCCDI) (WMO 2009). These extreme indices unfold the frequency, amplitude and persistence of extreme temperature and rainfall events. In this study area, twenty two indices (ten rainfall and twelve temperature extreme indices) are relevant to study the trend of future extreme rainfall and temperature values. The indices were calculated at each grid and at sub-basin level. The result of some of the indices is presented in Sect. 3.3. Daily observed and bias-corrected RCM rainfall, TMAX and TMIN for the near-term and long-term future periods were used to calculate the indices.

3 Results and discussion

3.1 Evaluation of bias correction methods

Linear scaling, power transformation and distribution mapping bias correction methods are effective in adjusting mean annual RCM simulation of rainfall. A substantial difference was found between raw RCM output and RCM output with bias correction in magnitude and spatial distribution of rainfall in the Jemma sub-basin (Fig. 4). The overestimation (CCLM model groups) and underestimation (REMO model groups) of annual rainfall outputs compared to the observed annual rainfall were sufficiently corrected for the entire sub-basin using linear scaling, power transformation and distribution mapping methods. These bias correction methods resounded comparable performance in adjusting mean annual rainfall of RCM outputs with the observed rainfall of the sub-basin (Fig. 4).

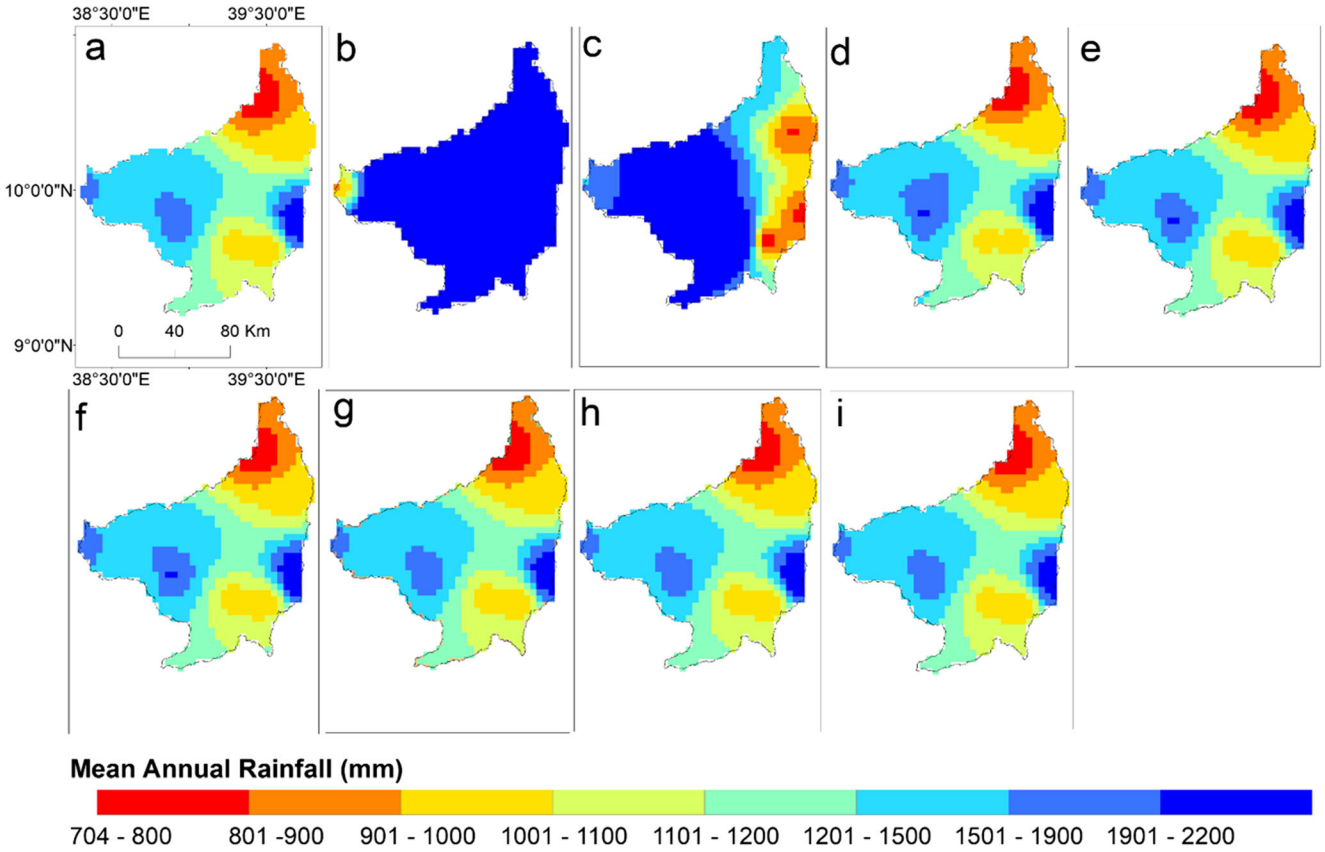

Fig. 4 Mean annual rainfall (mm) of observed, raw RCM simulations and bias-corrected RCM outputs for the period 1981–2005: (a) observation, (b) raw simulation of CCLM4 (CNRM-CM5), (c) raw simulation of REMO (EC-EARTH), (d) bias-corrected output of CCLM4 (CNRM-CM5) using distribution mapping, (e) bias-corrected output of REMO (EC-EARTH) using distribution mapping, (f) bias-corrected output of CCLM4 (CNRM-CM5) using linear scaling, (g) bias-corrected output of REMO (EC-EARTH) using linear scaling, (h) bias-corrected output of CCLM4 (CNRM-CM5) using power transformation (PT) and (i) bias-corrected output of REMO (EC-EARTH) using power transformation (PT)

Another important improvement of using bias correction methods in this study is in adjusting elevation dependent biases of RCM rainfall simulation. At the high elevation areas (> 2800 m) of the Jemma sub-basin, RCM simulation showed an overestimation of mean annual rainfall (Worku et al. 2018b). Conversely, in the lower elevation areas (< 1800 m) of the Jemma sub-basin, the RCM simulation is characterized by underestimation of mean annual rainfall. Such underestimation and overestimation of RCM simulation are effectively adjusted through all bias correction methods (Fig. 5). The overestimation of rainfall in high elevation areas by climate models simulation is not only in this study area. The simulation of rainfall by climate models was also characterized by overestimation over the Ethiopian highlands and the Upper Blue Nile Basin (Haile and Rientjes 2015). Probably, this could be due to the weakness of the models in the parametrization of local scale convection schemes and cloud parametrization in the high elevation areas.

Similar to annual rainfall simulation, the RCM simulation presented an overestimation and underestimation of mean monthly rainfall in the higher and lower elevation areas, respectively. The RCMs also provided different estimates of peak rainfall values at different locations in the sub-basin. The highest observed monthly rainfall occurred in July and August, whereas CCLM (CNRM-CM5) and CCLM (EC-EARTH) RCMs simulated higher rainfall occurred in September, October and May. Linear scaling, power transformation and distribution mapping methods were effective and showed comparable performance to correct the RCM simulation of mean monthly and seasonal rainfall biases. Sub-basin wide analysis showed that the RMSE and NSE between monthly observed rainfall and ensemble of RCM simulation of rainfall were 60 mm and 0.57, respectively. However, the RMSE and NSE between monthly observed rainfall and bias-corrected ensemble of RCM rainfall were 1.82 mm and 0.99, respectively.

Other studies (Teutschbein and Seibert 2012; Chen et al. 2013; Fang et al. 2015) have also investigated comparable performance among different bias correction methods in correcting mean monthly and annual rainfall and temperature values. For instance, power transformation, linear scaling, variance scaling and distribution mapping methods were

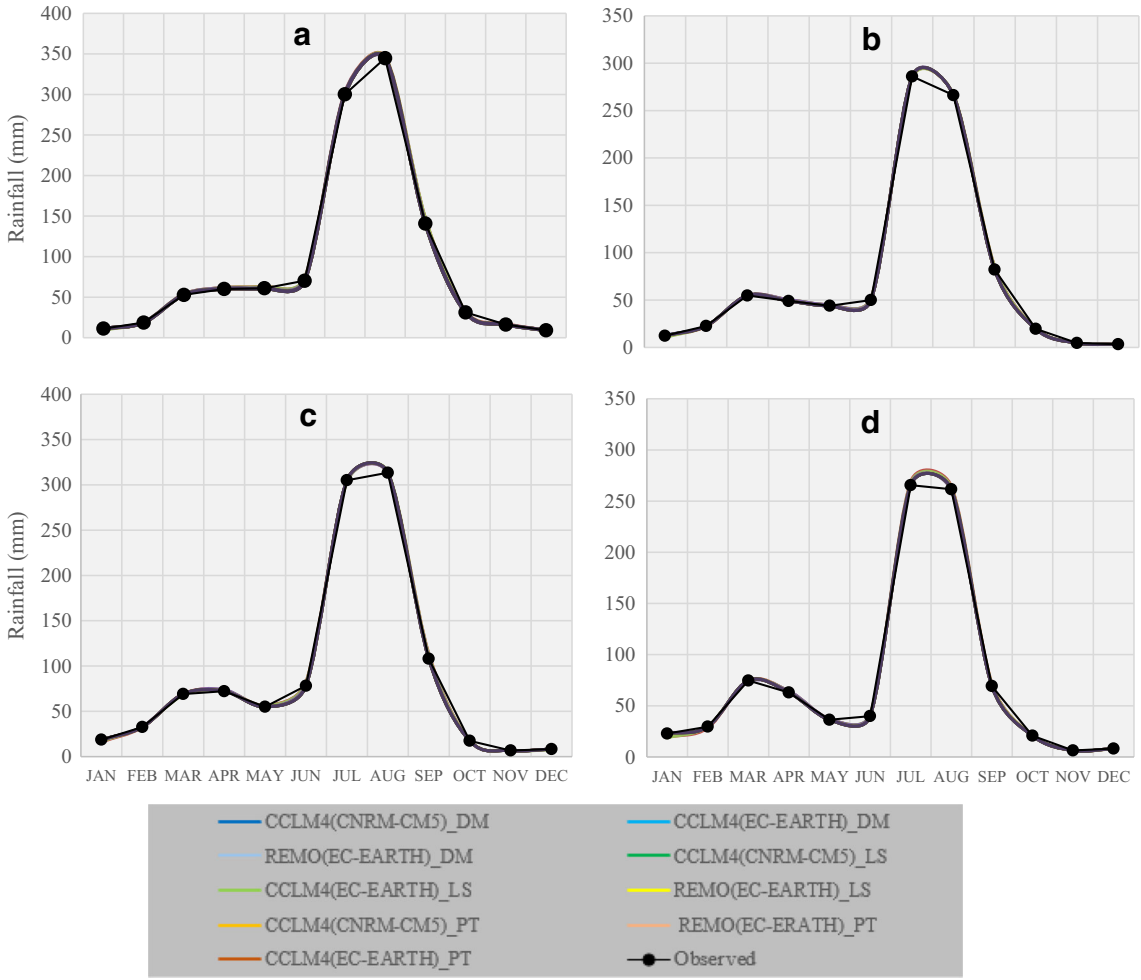

Fig. 5 Mean monthly rainfall (mm) of observed and bias-corrected RCMs in central (A),eastern (B), western (C) and northeastern (D) parts of the Jemma sub-basin. DM, LS and PT are to indicate distribution mapping, linear scaling and power transformation bias correction methods, respectively

successfully correct the mean values (Teutschbein and Seibert (2012). In the Upper Blue Nile Basin, bias correction methods showed improved performance in reproducing monthly rainfall values of GCM and RCM simulation (Elshamy et al. 2009; Liersch et al. 2016). Linear scaling bias correction method was also used to correct biases from Climate Forecast System Re-Analysis (CFSR) dataset and able to adjust mean daily, monthly and annual rainfall of the reanalysis dataset at different regions of Ethiopia (Berhanu et al. 2016).

The RCM simulation of temperature showed consistent underestimation. For example, the RCMs provided a consistent underestimation of mean monthly TMAX and TMIN in the central and higher elevation (north-eastern) areas of the sub-basin. Linear scaling, variance scaling and distribution mapping methods were effective and showed comparable performance in adjusting the RCM simulation of mean monthly TMAX and TMIN temperature. An illustration is available at S2 of supplementary information. Analogously, distribution mapping method was effective to adjust TMAX and TMIN simulation of GCMs at Addis Ababa, Ethiopia (Feyissa et al. 2018).

The high performance of bias correction methods in adjusting mean monthly and annual rainfall and temperature values unfolds most bias correction methods apply similar scale parameters to adjust the simulation of RCMs. The performance of bias correction methods in correcting the frequencies and intensities of rainfall and temperature events and values is to be evaluated using other robust statistical metrics. These are the extreme events of rainfall and temperature which trigger a higher impact on the socio-economic and natural ecosystems. As a result, climate scenarios that efficiently simulate extreme values are important to develop vigorous adaptation decisions.

Standard deviation, CV, percentiles and probability of wet days (P_{wet}) are robust statistical metrics to evaluate bias correction methods performance in fine-tuning extreme values and distribution of rainfall and temperature events. The three bias correction methods showed comparable performance in adjusting the CV of rainfall of the RCMs with the observed data. In all methods, there is a high CV during dry months (October–February) (Fig. 6). There exists an apparent

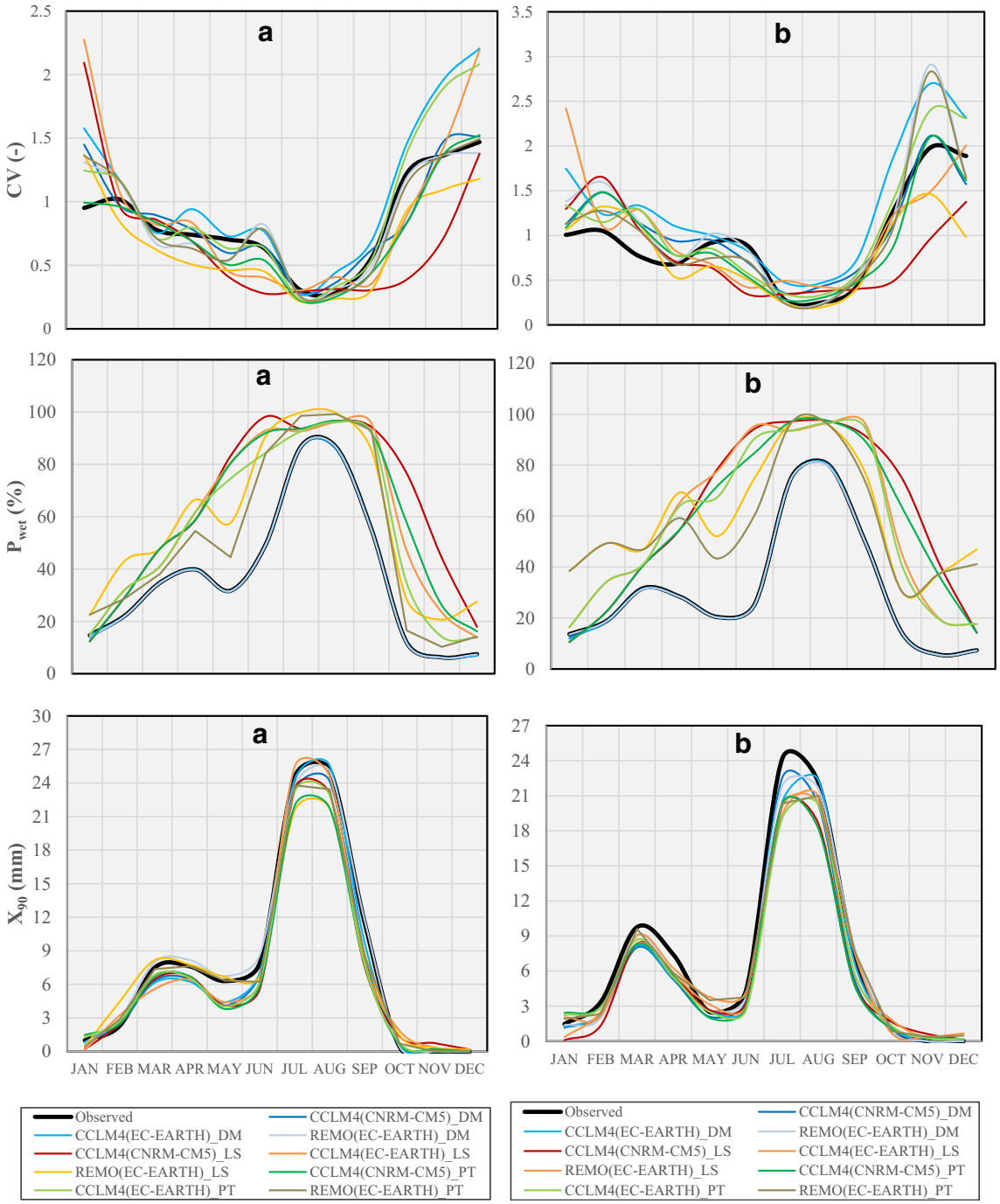

Fig. 6 Ability of linear scaling (LS), distribution mapping (DM) and power transformation (PT) to adjust the daily rainfall as measured by coefficient of variation (CV), 90th percentile (X_{90}) and probability of wet days (P_{wet}) in central (A) and northeastern (B) areas of the Jemma sub-basin

difference between distribution mapping, power transformation and linear scaling methods to adjust wet day probability. Distribution mapping method is better in reproducing wet day probability since it uses an RCM-specific rainfall threshold approach (Schmidli et al. 2006). There were drizzle rainfall events in all RCM simulation, which cause higher wet day probability in RCM rainfall simulations than observational rainfall. These drizzle rainfall events were effectively corrected with distribution mapping than linear scaling method and power transformation (Fig. 6). Outputs from the distribution mapping were also able to capture the 90th percentile of rainfall, particularly in the main rainy season, better than linear scaling and power transformation outputs (Fig. 6).

The 90th percentile of TMAX and TMIN were corrected well by linear scaling, variance scaling and distribution mapping methods, although distribution mapping performs better.

Table 2 Root mean square error (RMSE) between observation and simulation using bias correction methods during validation. In first case, the dry years were used for calibration and wet years were used for validation, and the second case vice versa

Validation years	Methods	Jan	Feb	Mar	Apr	May	Jun	Jul	Aug	Sep	Oct	Nov	Dec
Wet years	Linear scaling	135.51	87.54	83.80	3.63	35.03	50.09	55.33	115.98	29.66	22.15	101.53	152.70
	Distribution mapping	19.16	29.11	50.55	21.61	38.71	48.96	64.17	132.46	31.47	20.11	66.68	5.74
Dry years	Linear scaling	13.80	17.86	43.37	3.30	76.33	120.51	32.00	76.12	33.55	23.51	12.32	11.77
	Distribution mapping	13.98	18.25	44.53	1.62	73.29	118.59	34.57	79.94	31.04	22.13	12.60	11.87

Generally, the raw RCM simulations are characterized by underestimation of TMAX and TMIN. The distribution mapping method effectively corrected such deviations from the observational dataset. It particularly corrected the TMAX and TMIN better in the months of June to August compared to power transformation and linear scaling. An illustration is available on S3 of supplementary information.

Similar to this study, other studies (Teutschbein and Seibert 2012; Chen et al. 2013; Fang et al. 2015; Azmat et al. 2018) have also investigated a difference among bias correction methods in correcting standard deviations, wet day probability, percentiles and other extreme values. Distribution mapping method generally showed better performance in adjusting wet-day probability and percentiles of rainfall and temperature (Teutschbein and Seibert 2012; Fang et al. 2015; Azmat et al. 2018). For instance, Teutschbein and Seibert (2012) have identified that the distribution mapping method was better in correcting standard deviation, wet-day frequencies and 90th percentile than linear scaling, power transformation, variance scaling. Azmat et al. (2018) also investigated that distribution mapping method was better in 95th percentile, 5-day maximum rainfall (mm), maximum dry and wet spell length than local intensity scaling method.

Table 3 Future mean rainfall (mm) for the near-term (2021–2050) and long-term (2071–2100) periods compared to observed rainfall (1981–2005)

Scenario	RCMs	Mean annual rainfall (mm)	
		2021–2050	2071–2100
RCP4.5	Observed (1981–2005)	1001	1001
	CCLM(CNRM-CM5)	516 (−48%)	581 (−42%)
	CCLM(EC-EARTH)	788 (−21%)	740 (−26%)
	CCLM(MPI-ESM-LR)	828 (−18%)	782 (−22%)
	CCLM(HadGEM2-ES)	711 (−29%)	659 (−34%)
	REMO(EC-EARTH)	915 (−9%)	997 (−1%)
	REMO(MPI-ESM-LR)	1038 (2%)	984 (−2%)
	Ensemble mean	799 (−20%)	791 (−21%)
RCP8.5	CCLM(CNRM-CM5)	571 (−43%)	583 (−42%)
	CCLM(EC-EARTH)	666 (−34%)	703 (−30%)
	CCLM(MPI-ESM-LR)	808 (−20%)	804 (−20%)
	CCLM(HadGEM2-3S)	647 (−36%)	650 (−35%)
	REMO(EC-EARTH)	993 (−1%)	1135 (12%)
	REMO(MPI-ESM-LR)	1006 (0.5%)	985 (−2%)
	Ensemble mean	782 (−22.68%)	812 (−19%)
RCP2.6	REMO(EC-EARTH)	881 (−13%)	917 (−9%)
	REMO(MPI-ESM-LR)	954 (−6%)	947 (−6%)
	Ensemble mean	917 (−9%)	932 (−8%)

Therefore, it is commendable to use distribution mapping bias corrected rainfall and temperature RCM outputs for future climate change analysis and impact assessment. Such robust RCM outputs can be useful to develop climate change adaptation and mitigation strategies, such as devising sustainable watershed management practices that help to cope the challenges of climate change while building resilience (Dile et al. 2013). However, it is hardly known how these bias correction methods perform under climate condition, which is different from the current climate. Consequently, the performance of bias correction methods under different climate conditions is to be evaluated before using the output of bias correction methods for further climate change impact study.

The validation of bias correction methods using differential split sampling testing shows the bias correction algorithms can work under different climate condition, and this indicates that the correction methods are valid for future climate condition. During validation, the skill of bias correction methods is not as high as the performance during calibration. There are overestimation and underestimation at dry and rainy months under all bias correction methods during validation using the wet years' case. Using wet and dry years, the root mean square error (RMSE) during validation showed variation than during calibration. Still, the distribution mapping method is better than power transformation and linear scaling in producing monthly rainfall pattern and the RMSE of monthly rainfall is low under the distribution mapping method during validation using wet years (Table 2). Concurrently, Teutschbein and Seibert 2013 also identified that the distribution mapping method is better than other bias correction methods which unfold low deviation from observation and robust under changing climate conditions.

3.2 Projections of future rainfall and temperature

Future rainfall, TMAX and TMIN were projected using the outputs of RCM bias-corrected through distribution mapping

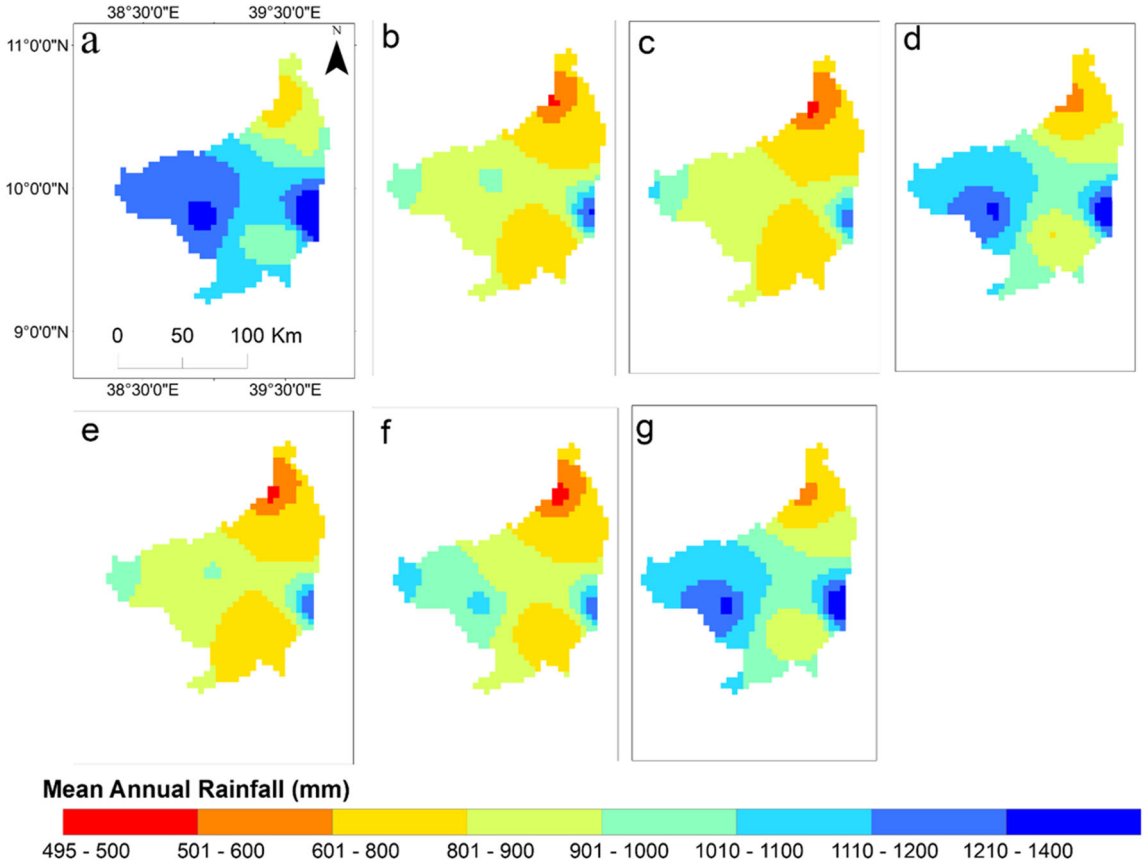

Fig. 7 Future models ensemble rainfall (mm) in comparison with observed rainfall: (a) observed, (b) ensemble mean (2021–2050) RCP4.5, (c) ensemble mean (2021–2050) RCP8.5, (d) ensemble mean (2021–2050) RCP2.6, (e) ensemble mean (2071–2100) RCP4.5, (f) ensemble mean (2071–2100) RCP8.5 and (g) ensemble mean (2071–2100) RCP2.6

method. Near-term (2021–2050) and long-term (2071–2100) future rainfall and temperature based on RCP4.5, RCP8.5 and RCP2.6 emission scenarios were compared with historical observed climate (1981–2005) (Table 3). The near-term and

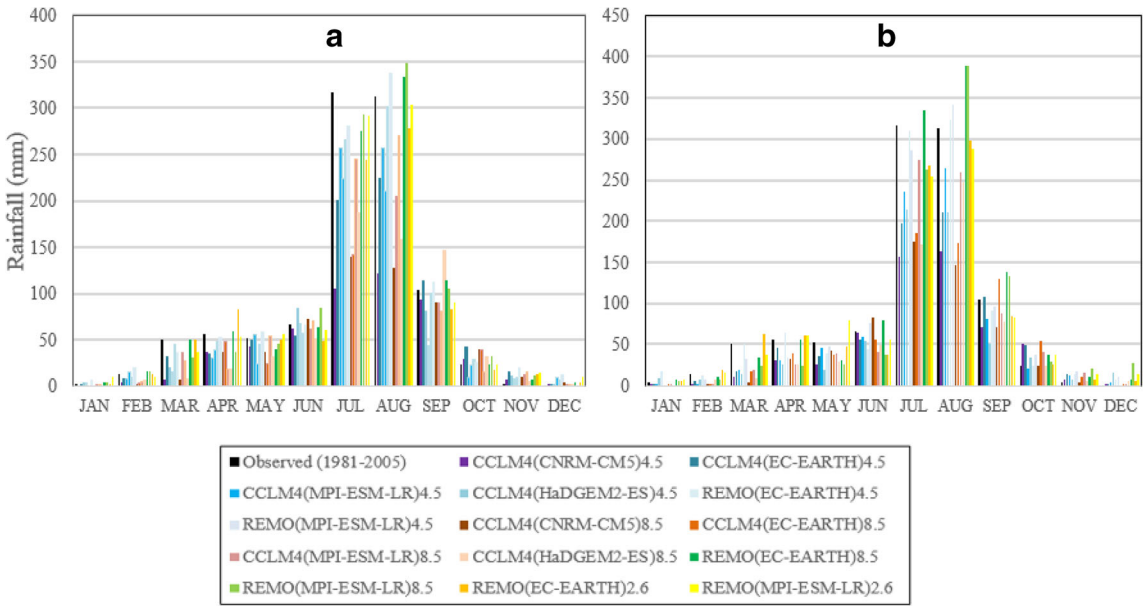

Fig. 8 Mean monthly observed (1981–2005) and (A) near-term (2021–2050) and (B) long-term (2071–2100) future mean monthly rainfall under RCP8.5, RCP4.5 and RCP2.6 emission scenarios. Values are area-weighted across the Jemma sub-basin

Table 4 Future and observed mean maximum and minimum temperature (°C)

Scenario	RCMs	Mean annual TMAX (°C)		Mean annual TMIN (°C)	
		2021–2050	2071–2100	2021–2050	20,171–2100
RCP4.5	Observed (1981–2005)	21.16	21.16	9.83	9.83
	CCLM(CNRM-CM5)	22.04 (+0.88)	22.99 (+1.83)	10.82 (+0.99)	12.14 (+2.30)
	CCLM(EC-EARTH)	22.28 (+1.11)	23.09 (+1.93)	11.11 (+1.27)	12.34 (+2.50)
	CCLM(MPI-ESM-LR)	22.19 (+1.02)	22.88 (+1.72)	11.14 (+1.30)	12.17 (+2.34)
	CCLM(HadGEM2-ES)	22.17 (+1.00)	23.33 (+2.17)	10.44 (+0.61)	11.75 (+1.92)
	REMO(EC-EARTH)	22.28 (+1.12)	23.08 (+1.91)	11.17 (+1.33)	12.53 (+2.70
	REMO(MPI-ESM-LR)	22.07 (+0.91)	23.04 (+1.8)	11.17 (+1.33)	12.34 (+2.50)
	Ensemble mean	22.17 (+1.01)	23.07 (+1.9)	10.97 (+1.14)	12.21 (+2.38)
RCP8.5	CCLM(CNRM-CM5)	22.15 (+0.99)	24.46 (+3.30)	11.13 (+1.30)	14.24 (+4.41)
	CCLM(EC-EARTH)	22.55 (+1.39)	21.79 (+0.63)	11.44 (+1.60)	14.87 (+5.04)
	CCLM(MPI-ESM-LR)	22.54 (+1.37)	24.81 (+3.64)	11.47 (+1.63)	15.07 (+5.23)
	CCLM(HadGEM2-ES)	22.41 (+1.25)	24.69 (+3.53)	11.41 (+1.57)	14.25 (+4.41)
	REMO(EC-EARTH)	22.34 (+1.17)	24.74 (+3.57)	11.55 (+1.71)	15.11 (+5.28)
	REMO(MPI-ESM-LR)	22.48 (+1.31)	25.28 (+4.11)	11.58 (+1.75)	15.46 (+5.62)
	Ensemble mean	22.41 (+1.25)	24.29 (+3.13)	11.43 (+1.59)	14.83 (+5.00)
RCP2.6	REMO(EC-EARTH)	21.91 (+0.75)	22.00 (+0.84)	10.70 (+0.88)	10.86 (+1.03)
	REMO(MPI-ESM-LR)	21.92 (+0.76)	21.86 (+0.70)	10.83 (+1.00)	10.76 (+0.94)
	Ensemble mean	21.915 (+0.755)	21.93 (+0.77)	10.77 (+0.94)	10.81 (+0.98)

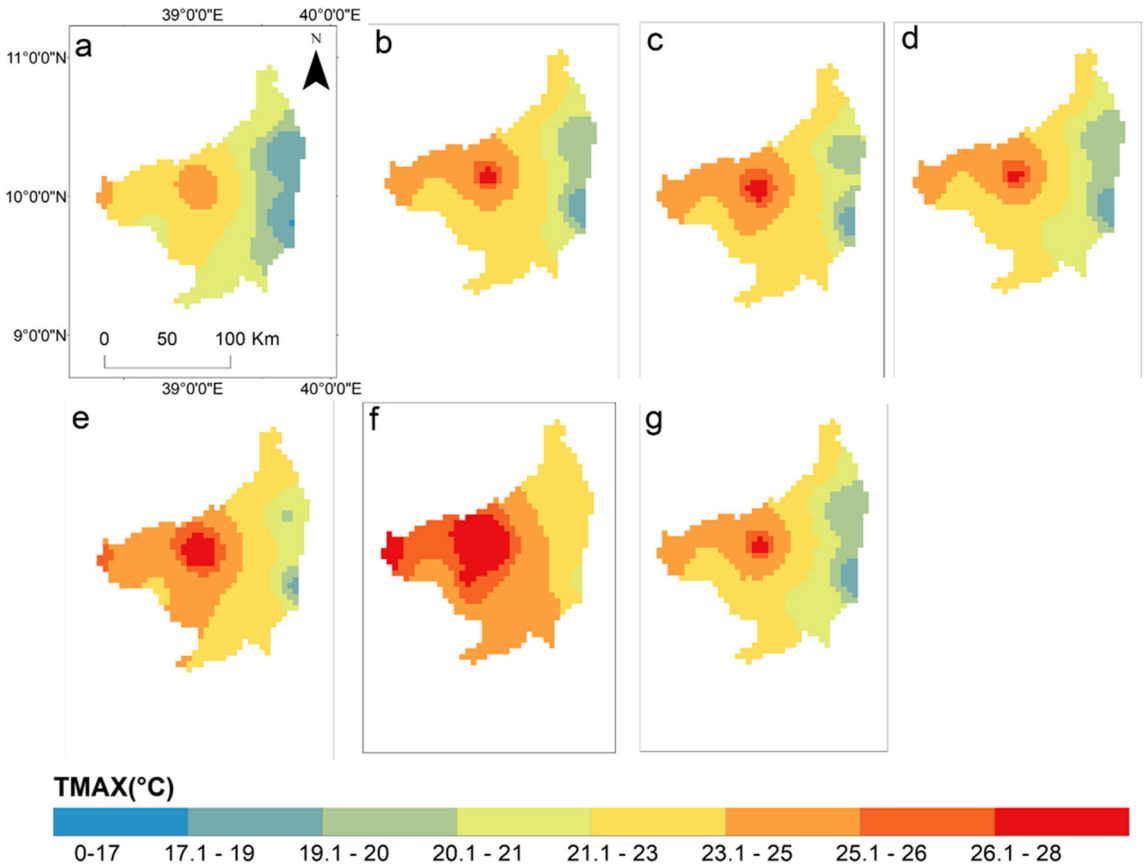

Fig. 9 Mean historical and future models ensemble maximum temperature (°C): (a) historical (1981–2005), (b) ensemble mean (2021–2050) RCP4.5, (c) ensemble mean (2021–2050) RCP8.5, (d) ensemble mean (2021–2050) RCP2.6, (e) ensemble mean (2071–2100) RCP4.5, (f) ensemble mean (2071–2100) RCP8.5 and (g) ensemble mean (2071–2100) RCP2.6

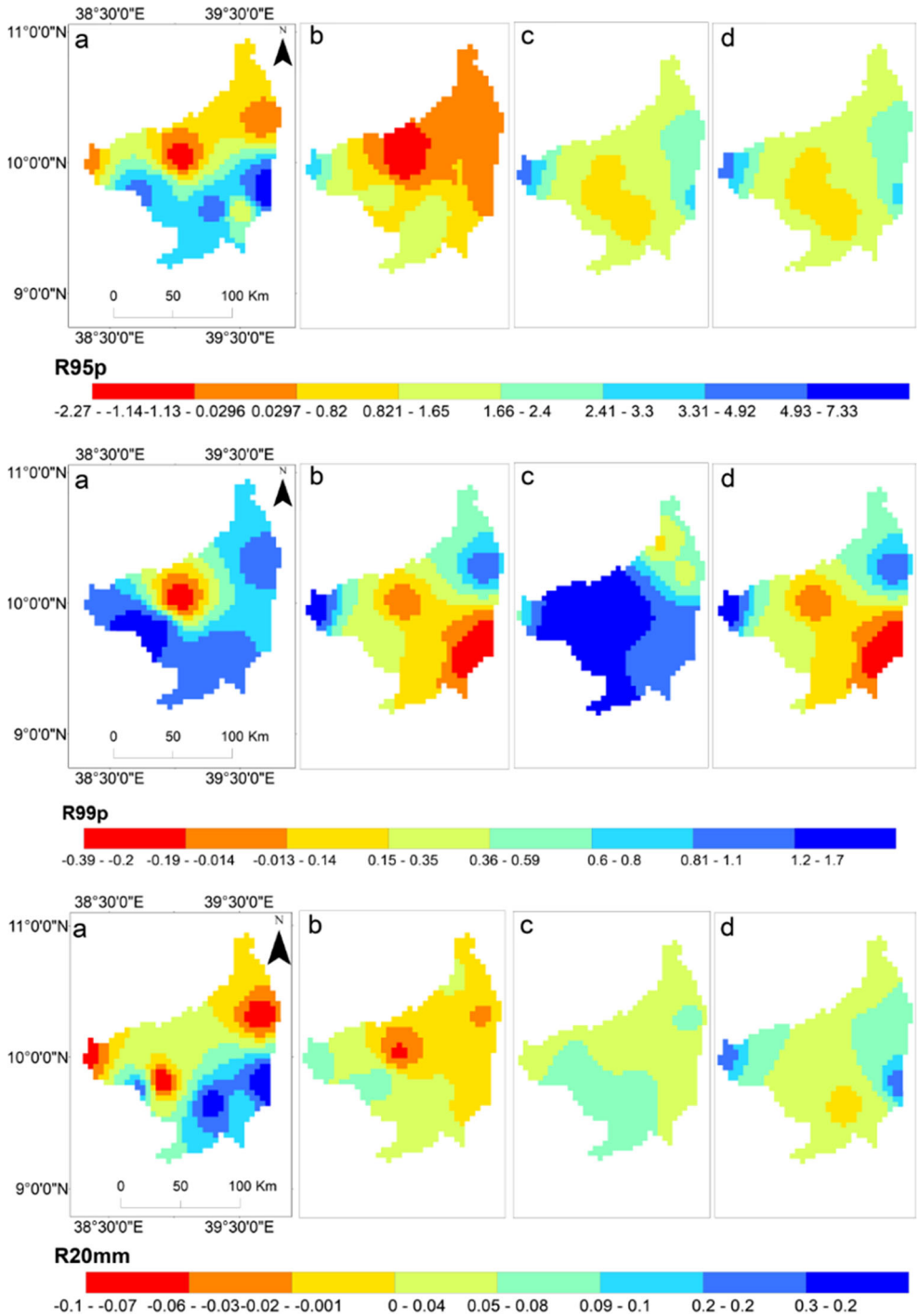

Fig. 10 Trends (mm/year) in R95p (very wet days), R99p (extreme wet days) and R20mm (number of very heavy precipitation days) in near future and long future from ensemble mean of RCMs: (a) observed (1981–2005), (b) ensemble mean (2021–2050) RCP4.5, (c) ensemble mean (2021–2050) RCP8.5 and (d) ensemble mean (2071–2100) RCP4.5

long-term annual rainfall of the Jemma sub-basin was projected to decrease under the RCP4.5, RCP8.5 and RCP2.6 emission scenarios, but with different magnitude. The ensemble of bias corrected RCM output showed 19% (or more) decline of rainfall for the near-term and long-term futures. The ensemble also showed that the decline in rainfall was higher in the near-term (− 22.68%) than long-term (− 19%) under the RCP8.5 scenario. While, under the RCP4.5 scenario, a higher decline of rainfall is projected for the long-term (− 21%) than the near-term future (− 20%). Lower reduction of rainfall in the near- and long-term future is projected under RCP2.6. However, when we compare similar RCMs under other emission scenarios (REMO (EC-EARTH) and REMO (MPI-ESM-LR)), there is comparable reduction of rainfall under RCP2.6 and other emission scenarios (Table 3).

Most of the individual RCMs (S-RCMs) projected a reduction of mean annual rainfall (Table 3) except REMO models. Individual RCM projection of future

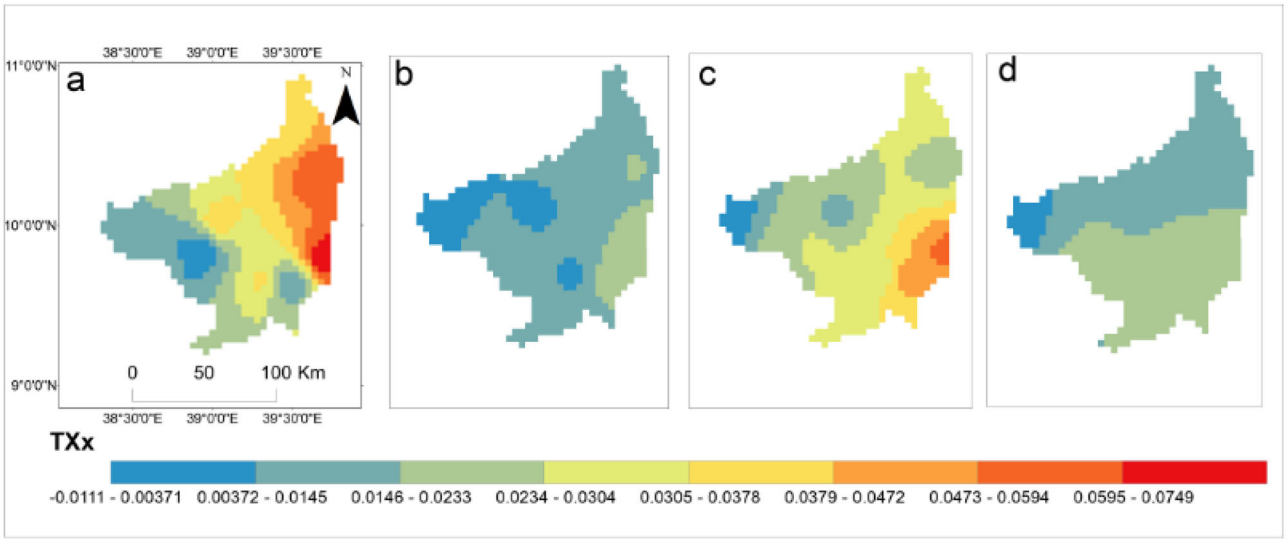
38°30'0"E
39°0'0"E
39°30'0"E
11°0'0"N
10°0'0"N
9°0'0"N
a
b
c
d
N
0
50
100 Km
TXx
-0.0111 - 0.00371
0.00372 - 0.0145
0.0146 - 0.0233
0.0234 - 0.0304
0.0305 - 0.0378
0.0379 - 0.0472
0.0473 - 0.0594
0.0595 - 0.0749

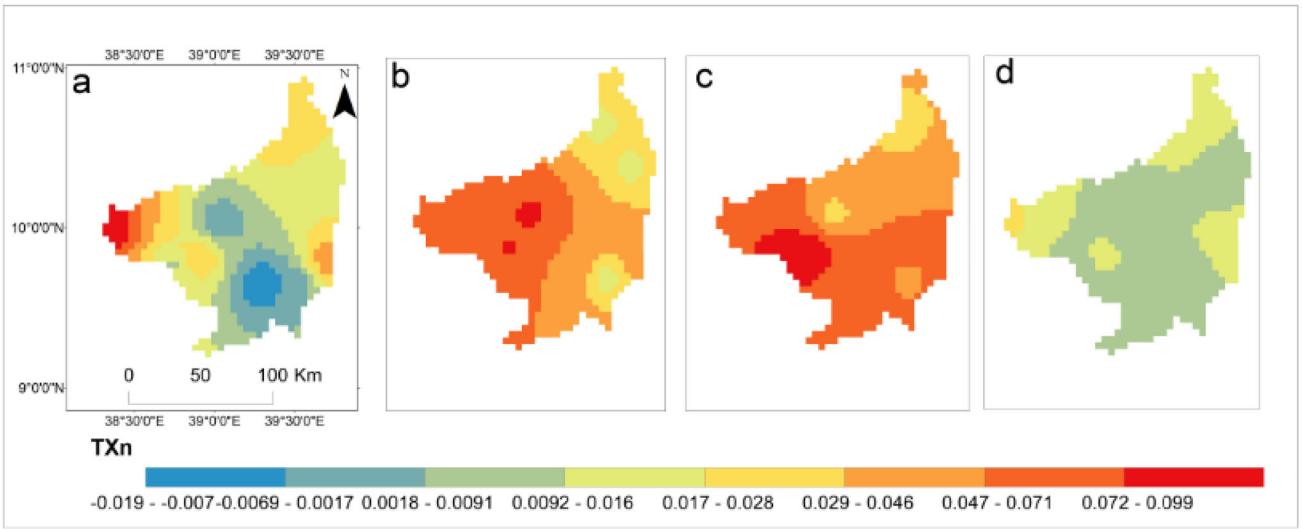
38°30'0"E
39°0'0"E
39°30'0"E
11°0'0"N
10°0'0"N
9°0'0"N
a
b
c
d
N
0
50
100 Km
TXn
-0.019 - -0.007
-0.0069 - 0.0017
0.0018 - 0.0091
0.0092 - 0.016
0.017 - 0.028
0.029 - 0.046
0.047 - 0.071
0.072 - 0.099

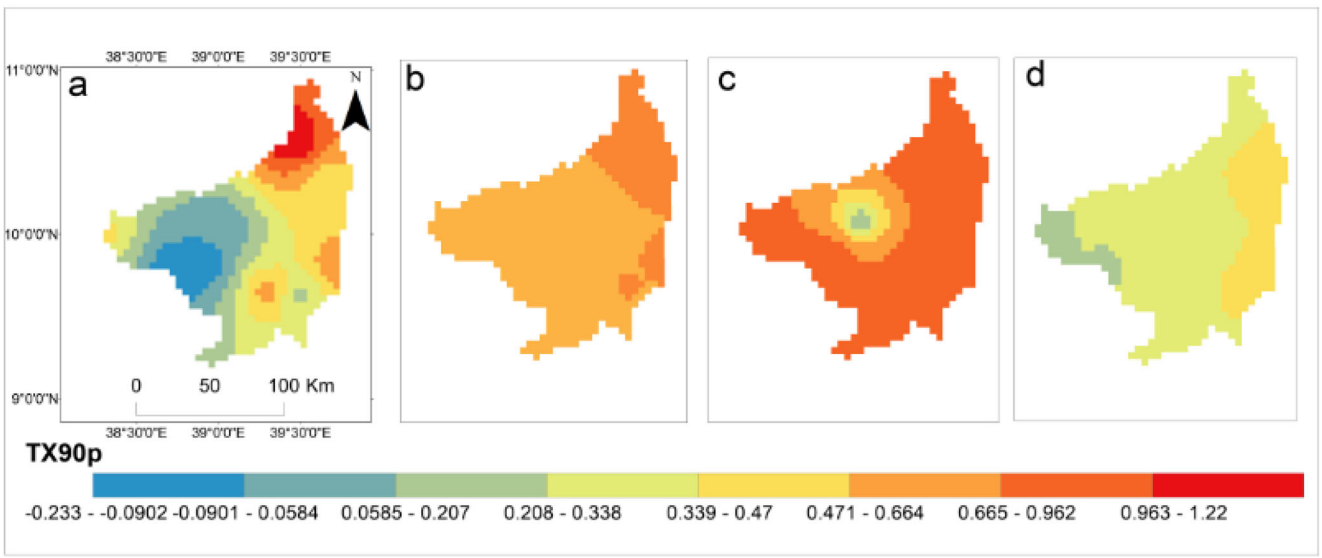
38°30'0"E
39°0'0"E
39°30'0"E
11°0'0"N
10°0'0"N
9°0'0"N
a
b
c
d
N
0
50
100 Km
TX90p
-0.233 - -0.0902
-0.0901 - 0.0584
0.0585 - 0.207
0.208 - 0.338
0.339 - 0.47
0.471 - 0.664
0.665 - 0.962
0.963 - 1.22

◀ **Fig. 11** Trends in TXx(Max TMAX, °C year^{-1}), TXn (Min TMAX, °C year^{-1}) and TX90p (warm days, % year^{-1}) in near future and far future from the ensemble mean of RCMs: (a) observed (1981–2005), (b) ensemble mean (2021–2050) RCP4.5, (c) ensemble mean (2021–2050) RCP8.5 and (d) ensemble mean (2071–2100) RCP4.5

rainfall ranged from −43% (CCLM (CNRM-CM5)) to 0.5% (REMO (MPI-ESM-LR)) for the near-term and from −42% (CCLM (CNRM-CM5)) to 12% (REMO (EC-EARTH)) for the long-term under RCP8.5 emission scenario. The projected future rainfall had the same spatial pattern with the observed rainfall, where lower rainfall is projected in the northern part of the sub-basin (Fig. 7).

The ensemble near-term and long-term mean monthly rainfall was also projected to decrease under RCP4.5, RCP8.5 and RCP2.6 emission scenarios. All RCM output showed a decrease in mean monthly rainfall in the near-term and long-term futures except GCMs downscaled using the REMO model (Fig. 8). Though the raw simulation of CCLM models was characterized by overestimation in simulating historical main rainy season (June–September) rainfall at higher altitudes (> 2800 m), higher monthly rainfall is projected from REMO models than CCLM models (Fig. 8).

Studies (e.g., Beyene et al. 2010; Dile et al. 2013) show a similar trend of rainfall in the Upper Blue Nile River basins in the future period. For example, Dile et al. (2013) found a decrease in rainfall by about −30% during 2010–2040 in Gilgel Abay watershed using statistically downscaled outputs of the HadCM3 model. Conversely, there are other studies (e.g., Mellander et al. 2013; Mekonnen and Disse 2016; Liersch et al. 2016) which project an increase in future rainfall in the Blue Nile Basin using GCM outputs. Mellander et al. (2013) projected an increase of mean annual rainfall by 6% in the Upper Blue Nile Basin from 2050 to 2100 using single ECHAM5/MP1-OM model output. Concomitantly, Mekonnen and Disse (2016) reported an increasing trend of future mean annual rainfall in this river basin using six GCM outputs under A1B, A2 and B1 scenarios. There are also other studies reported inconsistent or no trend of future rainfall (Elshamy et al. 2009; Setegn et al. 2011). Elshamy et al. (2009), using an ensemble of seventeen GCM outputs, showed almost no change in the future (2081–2098) annual rainfall in the Upper Blue Nile Basin. Likewise, Setegn et al. (2011) studied the hydro-meteorological change in the Lake Tana sub-basin using 11 CMIP3 GCM outputs. They found an inconsistent trend of future rainfall; of the eleven CMIP3 GCM outputs, nine of them indicated a decrease in rainfall.

Projected TMAX and TMIN showed an increasing trend under both RCP scenarios. Compared to the baseline period, in the near-term, future ensemble of models showed an increase of TMAX by 1.01 °C and TMIN by 1.14 °C under RCP4.5 scenario and an increase of TMAX by 1.25 °C and TMIN by 1.59 °C in RCP8.5 scenario. The highest increase was observed in the long-term future and for the RCP8.5 scenario, where the multi-model ensemble provided an increase of TMAX by 3.13 °C and TMIN by 5.00 °C (Table 4). Parallel to the assumption of emission scenarios, less increase of TMAX and TMIN is projected under RCP2.6 (Table 4). This substantiates that there will be low increase of temperature if the Paris Agreement and other substantial measures by the global society are realized. The projected future TMAX and TMIN showed a consistent spatial pattern with the observed TMAX and TMIN where lower values were projected in the eastern and northern part of the sub-basin (Fig. 9).

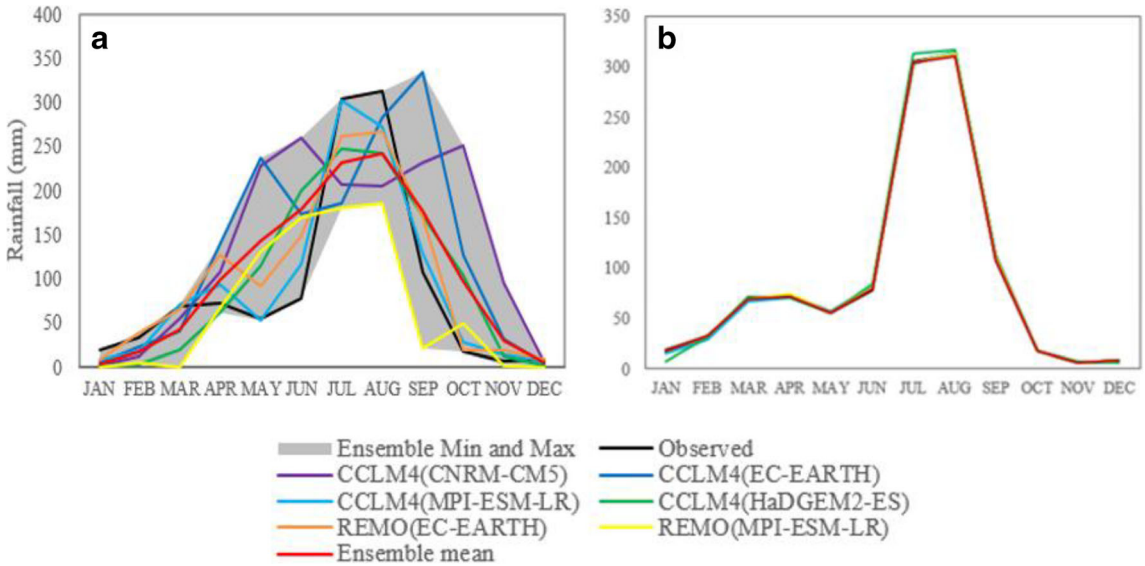

Fig. 12 The uncertainty width among the RCM simulation. (a) RCM simulation and (b) bias-corrected RCM output of mean monthly rainfall in comparison with observed rainfall for the historical period (1981–2005)

The findings of projected TMAX and TMIN trends in the Jemma sub-basin were also similar to other studies in the Blue Nile Basin (e.g. Elshamy et al. 2009; Liersch et al. 2016; Mekonnen and Disse 2016), and other regional and global reports (Beyene et al. 2010; IPCC 2013). For example, IPCC (2013) projected an increase in the mean temperature from 2081 to 2100 by 2.6 to 4.8 °C under the RCP8.5 scenario, which is comparable to the temperature trend estimated for the Jemma sub-basin. In the Blue Nile Basin, an increase in temperature in the future with different magnitude is projected from different models (Elshamy et al. 2009; Liersch et al. 2016; Mekonnen and Disse 2016).

3.3 Changes in future rainfall and temperature extremes

Analysis of changes in rainfall extremes in the near-term and long-term future using ETCCDI revealed that there would be an increase in rainfall extremes, which is contrary to the decreasing trend of future mean annual and monthly rainfall estimated in the sub-basin. In the near-term future under the RCP8.5 scenario, there will be a significant ($p < 0.05$) increase in the number of heavy rainfall days (R10mm) and very heavy rainfall days (R20mm). An increase of extreme wet-days (R99p) and very wet-days (R95p) is also projected, but not significant. In comparison with the trends of historical rainfall extremes (1981–2014) in the Jemma sub-basin (Worku et al. 2018a), an increasing trend of R20mm, R10mm and R95p is low, while the trend in extreme wet-days (R99p) is high than observed extreme rainfall trends (Fig. 10).

An increase in temperature extremes in the near-term and long-term future under both RCP scenarios in the entire sub-basin was projected (Fig. 11). All temperature indices showed an increase in temperature extreme events in the future climate. For instance, in the long-term future under RCP8.5 scenario, significant increasing trends are projected in TXx (Max TMAX), TXn (Min TMAX), TX90p (Warm days), TX10p (Cool days), TN10p (Cool nights) and TN90p (Warm nights) which confirm there would be more warming in the future. The magnitude of the trends in these temperature extreme indices is comparable with the historical trend of temperature extreme indices in the sub-basin (Worku et al. 2018a). Higher spatial homogeneity is observed in the trend of temperature extremes in future climate than trends of temperature extreme indices of historical climate, which is characterized by higher diversity among different areas of the sub-basin. Most temperature extremes indicate more warming trend in the future in the entire parts of the sub-basin (Fig. 11).

An increase in rainfall and temperature extremes is not only in our study, but there are also various studies which have investigated an increase of extremes in future climate. For instance, IPCC (2013) projected more frequent hot and fewer cold temperature extremes over most land areas of the world. Extreme rainfall events are projected to increase over different regions of North America at the end of the twenty-first century under RCP 8.5 scenario (Wang and Kotamarthi 2015). Specific to Ethiopia, Garland et al. (2015) estimated an increase in temperature extremes in the future over the highland regions of Ethiopia. TX_90P, TN_90P, TXx, TNx, TNn and Rx5day tend to increase in the future climate over Addis Ababa, central highlands of Ethiopia (Feyissa et al. 2018). In general, the future climate would be characterized by high rainfall and temperature extreme events and needs caution in designing adaptation structures.

3.4 Uncertainties

This study was based on blending of four GCMs (CNRM-CM5, EC-EARTH, HadGEM2-ES and MPI-ESM-LR), two RCMs (CCLM4 and REMO) and three emission scenarios (RCP2.6, RCP4.5 and RCP8.5). The consistency and uncertainties among RCMs and emission scenarios was also investigated. The observed rainfall was captured by the raw simulation of RCMs, and it is within the uncertainty range of rainfall simulated by different RCMs (Fig. 12). The ensemble mean of the RCMs is also within the uncertainty range of different RCM simulation and captures the pattern of mean monthly observed rainfall. Uncertainty could also stem from bias correction methods. In this study, bias correction did not trigger change on the climate change signal of rainfall. Both the raw RCM simulation and the bias-corrected outputs show comparable reduction of rainfall in main rainy season and an increase in autumn (September to October) season (see supplementary material). GCMs downscaled through REMO model showed a slight increase before and after bias correction.

The RCMs and the ensemble mean of RCMs showed uniformity in climate change signal, but with different magnitude. Strong similarity in rainfall change signal is found among the ensemble mean of the RCMs (E-RCMs) than among the individual RCM (S-RCM) simulations (Table 3). The GCMs downscaled through REMO model project lower reduction of rainfall in the future climate than GCMs downscaled by CCLM4 model. The difference among the RCMs to simulate rainfall could be attributed to the variation in the parametrization schemes used to represent sub-grid processes (local forcing) such as convective rainfall. Thus, RCM selection during climate scenario development could be crucial for climate change projection and climate change impact assessment.

The variation among emission scenarios is lower than the difference among the RCMs. In the RCP4.5 emission scenario, higher reduction of rainfall is projected in the long-term climate condition than the near-term climate condition. Conversely, higher reduction of rainfall is projected in the near-term than long-term climate condition under RCP8.5 emission scenario. This entails that emission scenarios could trigger changes in

some rainfall drivers, for instance emission scenarios may reduce convective activity and moisture of the lower atmosphere over the air fields of the Jemma sub-basin. This also accentuates local and regional forcings (internal variability) are to be also important drivers of rainfall of the Jemma sub-basin and the central highlands of Ethiopia. Another potential reason could be the variation in the projected tropical ocean warming in the near- and long-term future.

Considering the Paris agreement, future rainfall and temperature under RCP2.6 was also investigated. Rainfall projection has showed lower reduction under RCP2.6 emission scenarios. The RCMs (REMO(EC-EARTH) and REMO(MPI-ESM-LR)) under RCP4.5 and RCP8.5 also showed lower reduction of rainfall. This further emphasizes that larger uncertainty is found among the RCMs than the emission scenarios. However, it is not certain to achieve the Paris climate agreement which requires 10% reduction of emission by 2030 from 2015 level to realize a RCP2.6 and to limit warming to 2 °C above preindustrial level (Sanderson et al. 2016).

Contrary with the projected rainfall, large difference in projected TMAX and TMIN is observed among emission scenarios than among RCMs (Table 4). Corresponding with the projected concentration of greenhouse gases, high increase of TMAX and TMIN is projected in the long term future than the near term future and in the RCP8.5 than RCP4.5 and RCP2.6. Lower increases of TMAX and TMIN are projected under RCP2.6 emission scenario. The fifth IPCC assessment report has also attributed that emission scenarios are major drivers of temperature change (IPCC 2013). The individual RCMs and the ensemble mean of the RCMs project higher increase of TMIN than TMAX under near and long term climate scenarios. In general, the steady increase of TMAX and TMIN has showed strong agreement with the projected global temperature.

4 Conclusion

Statistical bias correction is essential to get reliable climate data from GCMs and RCMs for climate impact studies and subsequently climate change adaptations and mitigation policymaking. This study has intercompared statistical bias correction methods which ranges from some simple additive or multiplicative bias corrections methods to most robust distribution based bias correction methods using different statistical metrics. For this endeavour, rainfall and temperature simulations of six RCMs were used. The raw RCM simulations particularly GCMs downscaled using CCLM4 model were characterized by overestimation and underestimation of rainfall in the higher and lower elevation areas of the sub-basin, respectively. This bias of RCMs could stem from the initial boundary condition (GCMs) and RCMs convective cloud parametrization schemes. Thus, for other studies, it is worthwhile to use RCMs driven by reanalysis datasets such as ERA dataset to reduce uncertainties and to disentangle whether the biases are generated from RCMs or driving GCMs. This study was based on six RCMs; however, it is also important to use more number of RCMs to develop climate and climate impact scenarios.

This study ascertains a comparable performance among bias correction methods in reproducing mean monthly and mean annual rainfall and temperature. This unfolds as bias correction methods use similar scale parameters. However, most additive or multiplicative bias corrections methods struggle to adjust frequency based indices such as wet-day probability and the 90th percentiles. Distribution mapping method showed superior performance in adjusting wet-day probability and the 90th percentiles. Consequently, distribution mapping method is can be used to analyse extreme values like drought and flood and to design engineering structures to reduce impacts of extreme events. The performance of distribution mapping method to cope with non-stationary climate conditions also warrants as this method can be used in other sub-basins of the Blue Nile Basin. But, this study questions the use of linear scaling and power transformation to adjust RCM simulation and to develop climate scenarios. Further, future studies can be designed using other frequency based indices such as intensity of wet days, consecutive dry days, consecutive wet days and other indices to analyse the sensitivity of bias correction methods.

This study also develops climate scenarios using multiple GCMs and RCMs, emission scenarios and robust statistical bias correction method. Most individual RCMs (S-RCMs) and all ensemble mean of RCMs (E-RCMs) showed an agreement on climate change signal which revealed that the future climate will be characterized by drier condition and more warming. It is also projected that future climate will be characterized by extreme rainfall and temperature events. The change in climate and extremes events could trigger profound impacts on the natural and anthropogenic systems. To reduce anticipated impacts of climate change and extreme events, it is essential to develop and apply robust climate scenarios in designing optimal adaptation and mitigation structures in the Jemma sub-basin and other similar sub-basins of the Blue Nile Basin. Climate change and extreme values could also have compound impact through triggering flood or drought in the Jemma sub-basin. Therefore, it is important to simulate the impact of projected climate change on the hydrology of the Jemma sub-basin using well calibrated and validated hydrological model. Moreover, climate science and climate modelling are under continuous improvement that further increase climate models reliability and reduce uncertainty. Thus, climate scenario and climate impact scenarios can be refined in the future.

Acknowledgements The authors of this study are thankful to the Ethiopian National Meteorological Agency that kindly provided us with the daily weather data. The climate models data are downloaded from https://esg-dn1.nsc.liu.se/esgf-idp.

Funding information This study is financially supported by the first author from Addis Ababa University, Debretabor University and the Water and Land Resources Centre of Ethiopia. This study was also funded by the International Foundation for Science (IFS) (Grant No. W_6227-1).

References

Abdo KS, Fiseha BM, Rientjes THM, Gieske ASM, Haile AT (2009) Assessment of climate change impacts on the hydrology of Gilgel Abay catchment in Lake Tana Basin. Ethiopia Hydrol Process 23: 3661–3669

Adem AA, Tilahun SA, Ayana EK, Worqlul A.W, Assefa TT, Dessu SB, Melesse AM, (2016). Climate Change Impact on Stream Flow in the Upper Gilgel Abay Catchment, Blue Nile basin, Ethiopia. Landscape Dynamics, Soils and Hydrological Processes in Varied Climates 645–673. https://doi.org/10.1007/978-3-319-18787-7

Addor N, R€ossler O, K€oplin N, Huss M, Weingartner R, Seibert J (2014) Robust changes and sources of uncertainty in the projected hydrological regimes of Swiss catchments. Water Resour. Res., 50, 7541–7562. https://doi.org/10.1002/2013WR014132

Azmat M, Uzair M, Huggel C, Hussain E (2018) Future climate and cryosphere impacts on the hydrology of a scarcely gauged catchment on the Jhelum river basin, Northern Pakistan. Sci Total Environ. 639, 961–976. https://doi.org/10.1016/j.scitotenv.2018.05.206

Baldauf M, Seifert A, FöRstner J, Majewski D, Matthias R (2011) Operational convective-scale numerical weather prediction with the COSMO model : description and sensitivities. Am Meteorol Soc:3887–3905. https://doi.org/10.1175/MWR-D-10-05013.1

Berhanu B, Seleshi Y, Demisse SS, Melesse AM (2016) Bias correction and characterization of climate forecast system re-analysis daily precipitation in Ethiopia using fuzzy overlay 243, 230–243. Berhanu B, Seleshi Y, Demisse SS, Melesse AM (2016) Bias correction and characterization of climate forecast system re-analysis daily precipitation in Ethiopia using fuzzy overlay. Meteorol. Appl. 23:230–243. https://doi.org/10.1002/met.1549

Beyene T, Lettenmaier DP, Kabat P (2010) Hydrologic impacts of climate change on the Nile River basin : implications of the 2007 IPCC scenarios 2007–2008. https://doi.org/10.1007/s10584-009-9693-0

Chen J, Brissette P, Poulin A, Leconte R (2011) Overall uncertainty study of the hydrological impacts of climate change for a Canadian watershed 47:1–16. https://doi.org/10.1029/2011WR010602

Chen J, Brissette FP, Chaumont D, Braun M (2013) Finding appropriate bias correction methods in downscaling precipitation for hydrologic impact studies over North America. Water Resour Res 49:4187–4205. https://doi.org/10.1002/wrcr.20331

Christensen JH, Carter TR (2007) Evaluating the performance and utility of regional climate models : the PRUDENCE project. Climatic Change 81:1–6. https://doi.org/10.1007/s10584-006-9211-6

Conway D, Schipper ELF (2011) Adaptation to climate change in Africa : challenges and opportunities identified from Ethiopia. Glob Environ Chang 21:227–237. https://doi.org/10.1016/j.gloenvcha.2010.07.013

Cramér H (1999) Mathematical methods of statistics, ninth. edn. Princeton University Press

Dile YT, Berndtsson R, Setegn SG (2013) Hydrological response to climate change for Gilgel Abay River, in the Lake Tana Basin - upper Blue Nile Basin of Ethiopia. PLoS One 8:12–17. https://doi.org/10.1371/journal.pone.0079296

Doms G, Förstner J, Heise E, Herzog H-J, Mironov D, Raschendorfer M, Reinhardt T, Ritter B, Schrodin R, Schulz J-P, Vogel G (2011) COSMO II: Physical Parameterizations

Dosio A, Jürgen H, Schubert M, Daniel F (2015) Dynamical downscaling of CMIP5 global circulation models over CORDEX - Africa with COSMO - CLM : evaluation over the present climate and analysis of the added value. Clim Dyn 44:2637–2661. https://doi.org/10.1007/s00382-014-2262-x

Edwards PN (2011) History of climate modeling. WIREs Clim Change 2: 128–139. https://doi.org/10.1002/wcc.95

Elshamy ME, Seierstad IA, Sorteberg A (2009) Impacts of climate change on Blue Nile flows using bias-corrected GCM scenarios. Hydrol Earth Syst Sci 13:551–565. https://doi.org/10.5194/hess-13-551-2009

Fang GH, Yang J, Chen YN, Zammit C (2015) Comparing bias correction methods in downscaling meteorological variables for a hydrologic impact study in an arid area in China. Hydrol Earth Syst Sci 19: 2547–2559. https://doi.org/10.5194/hess-19-2547-2015

Feyissa G, Gete Z, Woldeamlak B, Gebremariam E (2018) Downscaling of Future Temperature and Precipitation Extremes in Addis Ababa under Climate Change. Climate 6(3):58. https://doi.org/10.3390/cli6030058

Flato G, Marotzke J, Abiodun B, Braconnot P, Chou SC, Collins W, Cox P, Driouech F, Emori S, Eyring V, Forest C, Gleckler P, Guilyardi E, Jakob C, Kattsov V, And CR, Rummukainen M (2013) Evaluation of Climate Models. In: Stocker TF, Qin D, Plattner G-K, Tignor M, Allen SK, Boschung J, Nauels A, Xia Y, Bex V, Midgley PM (eds) Climate Change 2013: The Physical Science Basis. Contribution of Working Group I to the Fifth Assessment Report of the Intergovernmental Panel on Climate Change. Cambridge University Press, Cambridge

Fouquart Y, Bonnel B (1980) Computations of solar heating of the earth's atmosphere: A new parameterization.Beitr. Phys Atmos 53:35–62

Fowler HJ, Blenkinsop S, Tebaldi C (2007) Linking climate change modelling to impacts studies : recent advances in downscaling techniques for hydrological. Int J Climatol. https://doi.org/10.1002/joc.1556

Garland RM, Matooane M, Engelbrecht FA (2015) Regional Projections of Extreme Apparent Temperature Days in Africa and the Related Potential Risk to Human Health. Int. J. Environ. Res. Public Health 12:12577–12604. https://doi.org/10.3390/ijerph121012577

Gebrehiwot SG, Ilstedt U (2011a) Hydrological characterization of watersheds in the Blue Nile Basin, 15:11–20. https://doi.org/10.5194/hess-15-11-2011

Giorgi F, Jones C, Asrar GR (2009) Addressing climate information needs at the regional level : the CORDEX framework. WMO Bulletin 58:175–183

Gudmundsson L, Bremnes JB, Haugen JE, Engen-Skaugen T (2012) Technical note: downscaling RCM precipitation to the station scale using statistical transformations – a comparison of methods. Hydrol Earth Syst Sci 16:3383–3390. https://doi.org/10.5194/hess-16-3383-2012

Gutowski WJ, Giorgi F, Timbal B, Frigon A, Jacob D, Kang H, Raghavan K, Lee B, Lennard C, Nikulin G, Rourke EO, Rixen M (2016) WCRP COordinated Regional Downscaling EXperiment (CORDEX): a diagnostic MIP for CMIP6. Geosci Model Dev: 4087–4095. https://doi.org/10.5194/gmd-9-4087-2016

Haile AT, Rientjes T (2015) Evaluation of regional climate model simulations of rainfall over the upper Blue Nile basin. Atmos Res 161–162:57–64. https://doi.org/10.1016/j.atmosres.2015.03.013

Hurni H, Tato K, Zeleke G (2005) The Implications of Changes in Population , Land Use , and Land Management for Surface Runoff in the Upper Nile Basin Area of Ethiopia Basin of Ethiopia.

Mountain Research and Development 25(2):147–154. https://doi.org/10.2307/3674675

IPCC (2013) Climate Change 2013: The Physical Science Basis. Working Group I Contribution to the Fifth Assessment Report of the Intergovernmental Panel on Climate Change

Klemeš V (2016) Operational testing of hydrological simulation models. Hydrolog Sci J 31(1):13–24. https://doi.org/10.1080/02626668609491024

Leander R, Buishand TA (2007) Resampling of regional climate model output for the simulation of extreme river flows. Journal of Hydrology 332:487–496. https://doi.org/10.1016/j.jhydrol.2006.08.006

Lenderink G, Buishand A, van Deursen W (2007) Estimates of future discharges of the river Rhine using two scenario methodologies: direct versus delta approach. Hydrol Earth Syst Sci 11:1145–1159. https://doi.org/10.5194/hess-11-1145-2007

Liersch S, Tecklenburg J, Rust H, Dobler A, Fischer M, Kruschke T, Koch H, Hattermann FF (2016) Are we using the right fuel to drive hydrological models ? A climate impact study in the Upper Blue Nile. Hydrol Earth Syst Sci Discuss 1–34. https://doi.org/10.5194/hess-2016-422

Maraun D (2012) Nonstationarities of regional climate model biases in European seasonal mean temperature and precipitation sums. Geophys Res Lett 39:1–5. https://doi.org/10.1029/2012GL051210

Maraun D (2016) Bias correcting climate change simulations - a critical review. Curr Clim Change Rep 2:211–220. https://doi.org/10.1007/s40641-016-0050-x

Mearns LO, Sain S, Leung LR, Bukovsky MS, Mcginnis S, Biner S, Caya D, Arritt RW, Gutowski W, Takle E, Snyder M, Jones RG, Nunes AMB, Tucker S, Herzmann D, Mcdaniel L, Sloan L (2013) Climate change projections of the North American Regional Climate Change Assessment Program. Climatic Change 120(4):965–975. https://doi.org/10.1007/s10584-013-0831-3

Mekonnen DF, Disse M, (2016) Analyzing the future climate change of Upper Blue Nile River Basin (UBNRB) using statistical down scaling techniques. Hydrol. Earth Syst. Sci. Discuss. https://doi.org/10.5194/hess-2016-543

Mellander P, Gebrehiwot SG, Gardenas A, Bewket W, Bishop K (2013) Summer rains and dry seasons in the Upper Blue Nile Basin : the predictability of half a century of past and future spatiotemporal patterns. PLoS ONE 8:1–12. https://doi.org/10.1371/journal.pone.0068461

Moss RH, Edmonds JA, Hibbard KA, Manning MR, Rose SK, van Vuuren DP, Carter TR, Emori S, Kainuma M, Kram T, Meehl GA, Mitchell JFB, Nakicenovic N, Riahi K, Smith SJ, Stouffer RJ, Thomson AM, Weyant JP, Wilbanks TJ (2010) The next generation of scenarios for climate change research and assessment. Nature 463:747–756. https://doi.org/10.1038/nature08823

Nikulin G, Jones C, Giorgi F, Asrar G, Chner MB, Cerezo-Mota R, Christensen OB, Qué MD, Fernandez J, Nsler AH, Van Meijgaard IE, Samuelsson P, Sylla MB, Sushama L (2012) Precipitation climatology in an ensemble of CORDEX-Africa regional climate simulations. J Clim 25:6057–6078. https://doi.org/10.1175/JCLI-D-11-00375.1

Piani C, Weedon GP, Best M, Gomes SM, Viterbo P, Hagemann S, Haerter JO (2010) Statistical bias correction of global simulated precipitation.pdf. J Hydrol 395:199–215

Randall DA, Wood RA, Bony S, Colman R, Fichefet T, Fyfe J, Kattsov V, Pitman A, Shukla J, Srinivasan J, Stouffer RJ, Sumi A, Taylor KE (2007) Cilmate Models and Their Evaluation. In: Solomon S, Qin D, Manning M, Chen Z, Marquis M, Averyt KB, Tignor M, Miller HL (eds) Climate Change 2007: The Physical Science Basis. Contribution of Working Group I to the Fourth Assessment Report of the Intergovernmental Panel on Climate Change. Cambridge University Press, Cambridge

Rathjens H, Bieger K, Srinivasan R, Arnold JG (2016) CMhyd User Manual: Documentation for preparing simulated climate change data for hydrologic impact studies

Ritter B, Geleyn J-F (1992) A comprehensive rRadiation scheme for numerical and weather prediction models with potential application in Climate Simulations. American Meteorological Society 120:303–325

Rockel B, Will A, Hense A (2008) The regional climate model COSMO-CLM. Meteorologist Zeitschrift 17:347–348. https://doi.org/10.1127/0941-2948/2008/0309

Sanderson B, Tebaldi C, O'Neill B (2016) What would it take to achieve the Paris temperature targets? Geophys Res Lett 43:7133–7142. https://doi.org/10.1002/2016GL069563

Schmidli J, Frei C, Vidale PL (2006) Downscaling from GCM precipitation: a benchmark for dynamical and statistical downscaling methods. Int J Climatol 26:679–689. https://doi.org/10.1002/joc.1287

SCRP (2000) Area of Andit Tid, Shewa , Ethiopia : Long-term Monitoring of the Agricultural Environment 1982-1994. Centre for Development and Environment, University of Berne, Switzerland, in Association with The Ministry of Agriculture, Ethiopia

Setegn SG, Rayner D, Melesse AM, Dargahi B, Srinivasan R (2011) Impact of climate change on the hydroclimatology of Lake Tana Basin, Ethiopia. Water Resour Res 47:1–13. https://doi.org/10.1029/2010WR009248

Taye MT, Willems P, Block P (2015) Implications of climate change on hydrological extremes in the Blue Nile basin: a review. J Hydrol Reg Stud 4:280–293. https://doi.org/10.1016/j.ejrh.2015.07.001

Taylor K, Ronald EJ, Touffer SGAM (2012) An overview of CMIP5 and the experiment design. Bull Am Meteorol Soc 93(4):485–498. https://doi.org/10.1175/BAMS-D-11-00094.1

Tesso G, Emana B, Ketema M (2012) A time series analysis of climate variability and its impacts on food production in North Shewa zone in Ethiopia. Afr Crop Sci J 20:261–274

Teutschbein C, Seibert J (2012) Bias correction of regional climate model simulations for hydrological climate-change impact studies: review and evaluation of different methods. J Hydrol 456–457:12–29. https://doi.org/10.1016/j.jhydrol.2012.05.052

Teutschbein C, Seibert J (2013) Is bias correction of regional climate model (RCM) simulations possible for non-stationary conditions. Hydrol Earth Syst Sci 17:5061–5077. https://doi.org/10.5194/hess-17-5061-2013

Tiedtke M (1989) A comprehesive mass flux scheme for cumulus parameterization in large-scale models. Am J Meteorol Soc 117:1779–1800

UN (2015) Adoption of the Paris Agreement. Conference of the Parties to the United Nations Framework Convention on Climate Change. Geneva : UN

Van Vuuren DP, Edmonds J, Kainuma M, Riahi K, Thomson A, Hibbard K et al (2011) The representative concentration pathways: an overview. Clim Change 109:5–31. https://doi.org/10.1007/s10584-011-0148-z

Wang J, Kotamarthi VR (2015) High-resolution dynamically downscaled projections of precipitation in the mid and late 21st century over North America. Earth's Future 3:268–288. https://doi.org/10.1002/2015EF000304.Received

Wilby RL, Wigley TM (1997) Downscaling general circulation model output: a review of methods and limitations methods and limitations. Progress in Physical Geography 21:530–548. https://doi.org/10.1177/030913339702100403

WMO (World Meteorological Organization) (2009) Guidelines on: analysis of extremes in a changing climate in support of informed decisions for adaptation. Climate Data and Monitoring WCDMP-No. 72. Geneva, Switzerland

WMO (World Meteorological Organization) (2009) Guidelines on: analysis of extremes in a changing climate in support of informed decisions for adaptation. Climate Data and Monitoring WCDMP-No 72

Woldemeskel FM, Sharma A, Sivakumar B, Mehrotra R (2015) Quantification of precipitation and temperature uncertainties simulated by CMIP3 and CMIP5 models. J. Geophys. Res. Atmos. 107, 3–17. https://doi.org/10.1029/2002JD002155

Worku G, Teferi E, Bantider A, Dile YT (2018a) Observed changes in extremes of daily rainfall and temperature in Jemma Sub-Basin, Upper Blue Nile Basin, Ethiopia. Dyn Atmos Oceans 135:839–854. https://doi.org/10.1007/s00704-018-2412-x

Worku G, Teferi E, Bantider A, Dile YT, Taye MT (2018b) Evaluation of regional climate models performance in simulating rainfall climatology of Jemma sub-basin, upper Blue Nile Basin, Ethiopia. Dyn Atmos Oceans 83:53–63. https://doi.org/10.1016/j.dynatmoce.2018.06.002

Yang X, Wood EF, Sheffield J, Ren L, Zhang M, Wang Y (2018). Bias correction of historical and future simulations of precipitation and temperature for China from CMIP5 models bias correction of historical and future simulations of precipitation and temperature for China from CMIP5 models. J. Hydrometeorol. 19. https://doi.org/10.1175/JHM-D-17-0180.1

Zhang X and Yang F (2004) RClimDex (1.0): user manual 1–23. Climate Research Branch Environment Canada Downsview, Ontario Canada